Reductive Formation of Straight Linear Metal−Metal Bonded Tetranuclear Complexes X−M−Mo−Mo−M−X from $X_2M\cdots Mo-Mo\cdots MX_2$ Supported by Four Tridentate 6-Diphenylphosphino-2-pyridonate Ligands (M = Pd, Pt; X = Cl, Br, I)

Kazushi Mashima,*,† Hiroshi Nakano,‡ and Akira Nakamura*,‡

Contribution from the Department of Chemistry, Faculty of Engineering Science, Osaka University, Toyonaka, Osaka 560, Japan, and Department of Macromolecular Science, Faculty of Science, Osaka University, Toyonaka, Osaka 560, Japan

Received February 26, 1996[⊗]

Abstract: Straight linear tetranuclear complexes have been prepared by using pyphos ligand (pyphos = 6-diphenylphosphino-2-pyridonate), which has unique coordinating sites comprised of three kinds of elements, *i.e.*, phosphine, nitrogen, and oxygen atoms, in almost linear fashion. The starting complex is the quadruply bonded dinuclear molybdenum(II) complex, $Mo_2(pyphos)_4$ (**1**), which was prepared by the reaction of $Mo_2(OAc)_4$ with sodium salt of pyphos. Single crystal X-ray analysis revealed that **1** consists of quadruply-bonded Mo_2 and *trans*-arranged diphosphine at both axial position of Mo_2 core. Thus, transition metal can be expected to be placed at both axial positions of Mo_2 core. Thus, treatment of **1** with Pd(II) and Pt(II) complexes gave rise to tetranuclear complexes of the general formula, $Mo_2Pd_2X_4(pyphos)_4$ (**2**) and $Mo_2Pt_2X_4(pyphos)_4$ (**4**) (**a**: X = Cl; **b**: X = Br; **c**: X = I). Single crystal X-ray analysis of **2a**, **2b**, and **4a** revealed the structure of complexes **2** and **4** that consist of M(II)···MoMo···M(II) skeleton supported by four pyphos ligands. They have quadruply-bonded Mo_2 core and no bonding between a M(II) atom and a Mo atom. Treatment of **2** and **4** with reducing reagents, photoirradiation, or thermal reduction resulted in the formation of metal−metal bonded tetranuclear complexes $Mo_2Pd_2X_2(pyphos)_4$ (**6**) and $Mo_2Pt_2X_2(pyphos)_4$ (**7**) (**a**: X = Cl; **b**: X = Br; **c**: X = I), respectively. All of them were characterized by single crystal X-ray analysis, which revealed that they consist of M(I)-MoMo-M(I) skeleton supported by pyphos ligands. The bond lengths between M(I) and Mo are short enough to be formally regarded as a single M(I)-Mo bond, while the longer Mo−Mo distance compared to that of **1**, **2**, and **4** indicated that the Mo−Mo bond of **6** and **7** are formally triple ($\pi^2\delta$ component). The electrochemical study indicates that all the atoms in the M−Mo−Mo−M system are electronically strongly coupled to allow an effective 2-electron redox process, and thus the chemical reduction of **2** and **4** readily gives **6** and **7**, respectively.

Introduction

Low-dimensional materials have attracted much interest in view of their magnetic, electronic, and optical properties.[1−3] In this field, inorganic as well as organometallic compounds have been studied since they are the molecular precursors for constructing such materials. Although compounds containing a linear array of few metal atoms have been reported so far,[4−15] the polymerization of metal-to-metal multiple bond, similar to the polymerization of alkenes and alkynes, would be the most rational synthetic method to preparing one-dimensional transition-metal-based materials (eq 1), thereafter (*n*) and (*n*−1) denote the order of multiplicity of metal−metal bond, though this approach has been unsuccessful with oppressive difficulty.

† Faculty of Engineering Science, Osaka University.
‡ Faculty of Science, Osaka University.
⊗ Abstract published in *Advance ACS Abstracts,* September 1, 1996.

(1) (a) Williams, J. M. *Adv. Inorg. Chem. Radiochem.* **1983**, *26*, 235. (b) Böhn, M. C. *One-Dimensional Organometallic Materials*; Springer: 1987. (c) Laine, R. M. *Inorganic and Organometallic Polymers with Special Properties*; Kluwer Academic Publishers, Dordrecht, 1992. (d) Clark, R. J. H. *Chem. Soc. Rev.* **1990**, *19*, 107. (e) Schulz, H.; Lehmann, H.; Rein, M.; Hanack, M. *Structure and Bonding* **1990**, 74.

(2) (a) Marks, T. J. *Science* **1985**, *227*, 881. (b) Marks, T. J. *Angew. Chem., Int. Ed. Engl.* **1990**, *29*, 857.

(3) (a) Kahn, O. *Structure and Bonding* **1987**, *68*, 89. (b) Miller, J. S.; Epstein, A. J.; Reiff, W. M. *Chem. Rev.* **1988**, *88*, 201. (c) Canneschi, A.; Gatteschi, D.; Sessioli, R.; Rey, P. *Acc. Chem. Res.* **1989**, *22*, 392. (d) Guillou, O.; Kahn, O.; Oushoorn, R. L.; Boubekeur, K.; Batail, P. *Inorg. Chim. Acta* **1992**, *198*−200, 119.

(4) (a) Wang, S.; Garzón, G.; King, C.; Wang, J.-C.; Fackler, J. P., Jr. *Inorg. Chem.* **1989**, *28*, 4623. (b) Real, J.; Bayón, J. C.; Lahoz, F. J.; López, J. A. *J. Chem. Soc., Chem. Commun.* **1989**, 1998.

(5) (a) Cayton, R. H.; Chisholm, M. H. *J. Am. Chem. Soc.* **1989**, *111*, 8921. (b) Cayton, R. H.; Chisholm, M. H.; Huffman, J. C.; Lobkovsky, E. B. *Angew. Chem., Int. Ed. Engl.* **1991**, *30*, 862. (c) Cayton, R. H.; Chisholm, M. H.; Huffman, J. C.; Lobkovsky, E. B. *J. Am. Chem. Soc.* **1991**, *113*, 8709.

(6) Cayton, R. H.; Chisholm, M. H.; Drarrington, F. D. *Angew. Chem., Int. Ed. Engl.* **1990**, *29*, 1491.

(7) Some examples of trinuclear complexes: (a) Beck, J.; Strähle, J. *Angew. Chem., Int. Ed. Engl.* **1985**, *24*, 409. (b) Murray, H. H.; Briggs, D. A.; Garzón, G.; Raptis, R. G.; Porter, L. C.; Fackler, J. P., Jr. *Organometallics* **1987**, *6*, 1992. (c) Ni, J.; Fanwick, P. E.; Kubiak, C. P. *Inorg. Chem.* **1988**, *27*, 2017. (d) Sykes, A. G.; Mann, K. R. *J. Am. Chem. Soc.* **1990**, *112*, 7247. (e) Tsai, M.-S.; Peng, S.-M. *J. Chem. Soc., Chem. Commun.* **1991**, 514. (f) Che, C.-M.; Yip, H. K.; Li, D.; Peng, S.-M.; Lee, G.-H.; Wang, Y.-M.; Liu, S.-T. *J. Chem. Soc., Chem. Commun.* **1991**, 1615. (g) Batchelor, R. J.; Einstein, F. W. B.; Pomeroy, R. K.; Shipley, J. A. *Inorg. Chem.* **1992**, *31*, 3155. (h) Yang, E.-C.; Cheng, M.-C.; Tsai, M.-S.; Peng, S.-M. *J. Chem. Soc., Chem. Commun.* **1994**, 2377. (i) Carlson, T. F.; Fackler, J. P., Jr.; Staples, R. J.; Winpenny, R. E. P. *Inorg. Chem.* **1995**, *34*, 426.

(8) (a) Balch, A. L. *Pure Appl. Chem.* **1988**, *60*, 555. (b) Balch, A. L.; Catalano, V. J.; Chatfield, M. A.; Nagle, J. K.; Olmstead, M. M.; Reedy, J., P. E. *J. Am. Chem. Soc.* **1991**, *113*, 1252. (c) Balch, A. L. *Prog. Inorg. Chem.* **1994**, *41*, 239.

(9) (a) Lippard, S. J. *Science* **1982**, *218*, 1075. (b) Hollis, L. S.; Lippard, S. J. *J. Am. Chem. Soc.* **1983**, *105*, 3494. (c) Hollis, L. S.; Lippard, S. J. *Inorg. Chem.* **1983**, *22*, 2600. (d) O'Halloran, T. V.; Robert, M. M.; Lippard, S. J. *Inorg. Chem.* **1986**, *25*, 957.

S0002-7863(96)00606-3 CCC: $12.00

The chemistry of multiply-bonded dinuclear complexes, which are monomers in eq 1, has been developed for last two decade, and a great variety of the quadruply bonded dinuclear complexes including the δ bonding has been synthesized.[16,17] With an intent for assembling one-dimensional binary systems from organic and inorganic molecules, the interaction of multiply-bonded M_2 complexes with bidentate organic donor ligands has also been actively investigated (eq 2).[18−21] On the other hand, the direct metal-to-metal axial interaction among multiply bonded M_2 units (eq 3) has not been achieved.[5]

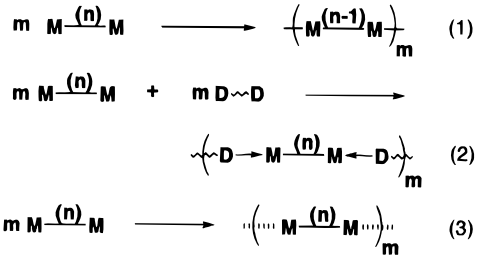

The multiply bonded M_2 complexes are now found to undergo a variety of the reactions cognate to that of carbon−carbon multiple bonds, namely, substitution, oxidative addition, reductive elimination, metathesis and [2 + 2] cycloaddition of metal−metal multiply bonded dinuclear complexes.[16,22]

We are interested in the reaction shown in eq 4, in which the addition of two metal atoms to the axial positions of a multiple metal−metal bond, as one of the preparative routes to metal chains.[23] For preparing the required complexes, it is strategically important to choose a ligand supporting metal atoms at the specified positions. Many multinuclear complexes have already been synthesized by using different kinds of bidentate ligands, *i.e.*, O−N bridging[9−11,24−28] and N−P bridging[8,29] ligands. We used a tridentate ligand of 6-diphenylphosphino-2-pyridonate (abbreviated pyphos), which has three coordination sites, O, N, and P, supported linearly by the rigid pyridone ring.[30] Thus, the pyphos ligand is found to be one of the most suitable ligands for arranging transition metals in linear manner. Here, we fully describe the syntheses and characterization of a dinuclear Mo_2 complex and then the tetranuclear complexes having specified linear structures, *e.g.*, M(II)···MoMo···M(II) and M(I)−MoMo−M(I) (M = Pd and Pt), supported by the pyphos ligands.

Results

Synthesis and Structure of Mo_2(pyphos)$_4$ (1). Dinuclear molybdenum(II) complex, Mo_2(pyphos)$_4$ (**1**) (pyphos = 6-diphenylphosphino-2-pyridonate), was obtained by the ligand exchange reaction of a quadruply-bonded dinuclear complex, $Mo_2(O_2CCH_3)_4$,[31] with 6-diphenylphosphino-2-pyridone (abbreviated as pyphosH) in the presence of sodium methoxide in dichloromethane (eq 5). The yellow color of the reaction mixture immediately turned red. Removal of sodium acetate followed by crystallization from dichloromethane−diethyl ether afforded **1** as red plates in 53% yield. The $^{31}P\{^1H\}$ NMR spectrum of **1** displayed a singlet at δ −7.8, indicating that four phosphorus atoms of the four pyphos ligands of **1** are equivalent in solution. The chemical shift value lies in the range of conventional triaryl-substituted phosphorus nuclei. Thus, the four phosphorus atoms are free from coordination to transition metal, and the dinuclear structure consists of bridged N and O chelation of the four pyphos ligands.

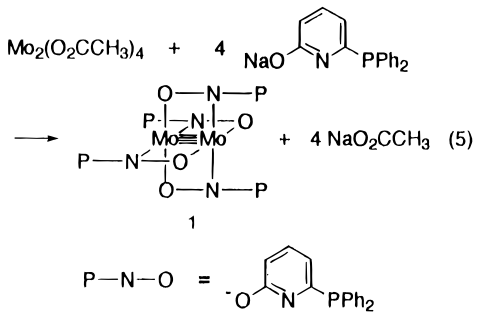

Figure 1 shows the crystal structure of **1**. Selected atomic distances and angles are given in Table 1. Complex **1**

(10) (a) Neugebauer, D.; Lippert, B. *J. Am. Chem. Soc.* **1982**, *104*, 6596. (b) Micklitz, W.; Müller, G.; Huber, B.; Riede, J.; Rashwan, F.; Heinze, J.; Lippert, B. *J. Am. Chem. Soc.* **1988**, *110*, 7084. (c) Micklitz, W.; Riede, J.; Huber, B.; Müller, G.; Lippert, B. *Inorg. Chem.* **1988**, *27*, 1979. (d) Lippert, B. *Prog. Inorg. Chem.* **1989**, *37*, 1. (e) Lippert, B.; Micklitz, W.; Renn, O.; Trötscher, G.; Dieter, I.; Frommer, G. *Pure Appl. Chem.* **1990**, *62*, 1075. (f) Trötscher, G.; Micklitz, W.; Schöllhorn, H.; Thewalt, U.; Lippert, B. *Inorg. Chem.* **1990**, *29*, 2541. (g) Renn, O.; Albinati, A.; Lippert, B. *Angew. Chem., Int. Ed. Engl.* **1990**, *29*, 84. (h) Micklitz, W.; Sheldrick, W. S.; Lippert, B. *Inorg. Chem.* **1990**, *29*, 211. (i) Schreiber, A.; Krizanovic, O.; Fusch, E. C.; Lippert, B.; Lianza, F.; Albinati, A.; Hill, S.; Goodgame, D. M. L.; Stratemeier, H.; Hitchman, M. A. *Inorg. Chem.* **1994**, *33*, 6101. (j) Wienkötter, T.; Sabat, M.; Fusch, G.; Lippert, B. *Inorg. Chem.* **1995**, *34*, 1022.

(11) (a) Matsumoto, K.; Fuwa, K. *J. Am. Chem. Soc.* **1982**, *104*, 897. (b) Matsumoto, K.; Takahashi, H.; Fuwa, K. *Inorg. Chem.* **1983**, *22*, 4086. (c) Sakai, K.; Matsumoto, K. *J. Am. Chem. Soc.* **1989**, *111*, 3074. (d) Matsumoto, K.; Sakai, K.; Nishio, K.; Tokisue, Y.; Ito, R.; Nishide, T.; Shichi, Y. *J. Am. Chem. Soc.* **1992**, *114*, 8110.

(12) Ciriano, M. A.; Sebastián, S.; Oro, L. A.; Tiripicchio, A.; Tiripicchio-Camellini, M.; Lahoz, F. J. *Angew. Chem., Int. Ed. Engl.* **1988**, *27*, 402.

(13) Elsevier, C. J.; Mul, W. P.; Vrieze, K. *Inorg. Chim. Acta* **1992**, *198−200*, 689.

(14) Lange, C. W.; Földeaki, M.; Nevodchikov, V. I.; Cherkasov, V. K.; Abakumov, G. A.; Pierpont, C. G. *J. Am. Chem. Soc.* **1992**, *114*, 4220.

(15) (a) Usón, R.; Laguna, A.; M., L.; Tartón, M. T.; Jones, P. G. *J. Chem. Soc., Chem. Commun.* **1988**, 740. (b) Usón, R.; Laguna, A.; M., L.; Jiménez, J.; Jones, P. G. *Angew. Chem., Int. Ed. Engl.* **1991**, *30*, 198. (c) Laguna, A.; M., L.; Jiménez, J.; Lahoz, F. J.; Olmos, E. *Organometallics* **1994**, *13*, 253. (d) Usón, R.; Forniés, J.; Tomás, M.; Ara, I. *Inorg. Chem.* **1994**, *33*, 4023.

(16) Cotton, F. A.; Walton, R. A. *Multiple Bonds between Metal Atoms*, 2nd ed.; Oxford University Press: 1993.

(17) Cotton, F. A. *Pure Appl. Chem.* **1992**, *64*, 1383.

(18) Cotton, F. A.; Felthouse, T. R. *Inorg. Chem.* **1980**, *19*, 328.

(19) Cotton, F. A.; Kim, Y.; Ren, T. *Inorg. Chem.* **1992**, *31*, 2723.

(20) (a) Kerby, M. C.; Eichhorn, B. W.; Creighton, J. A.; Vollhardt, K. P. C. *Inorg. Chem.* **1990**, *29*, 1319. (b) Eichhorn, B. W.; Kerby, M. C.;; Haushalter, R. C.; Vollhart, K. P. C. *Inorg. Chem.* **1990**, *29*, 723.

(21) (a) Handa, M.; Kasamatsu, K.; Kasuga, K.; Mikuriya, M.; Fujii, T. *Chem. Lett.* **1990**, 1753. (b) Handa, M.; Sono, H.; Kasamatsu, K.; Kasuga, K.; Mikuriya, M.; Ikenoue, S. *Chem. Lett.* **1992**, 453. (c) Handa, M.; Mikuriya, M.; Nukada, R.; Matsumoto, H.; Kasuga, K. *Bull. Chem. Soc. Jpn.* **1994**, *67*, 3125.

(22) (a) McGinnis, R. N.; Ryan, T. R.; McCarley, R. E. *J. Am. Chem. Soc.* **1978**, *100*, 7900. (b) Cotton, F. A.; Powell, G. L. *Inorg. Chem.* **1983**, *22*, 871. (c) Chisholm, M. H.; Clark, D. L.; Folting, K.; Huffman, J. C. *Angew. Chem., Int. Ed. Engl.* **1986**, *25*, 1014. (d) Carlin, R. T.; McCarley, R. E. *Inorg. Chem.* **1989**, *28*, 3432. (e) Chen, J.-D.; Cotton, F. A. *J. Am. Chem. Soc.* **1991**, *113*, 5857.

(23) Manners, I. *Chemistry in Britain* **1996**, 46.

(24) Cotton, F. A.; Fanwick, P. E.; Niswander, R. H.; Sekutowski, J. C. *J. Am. Chem. Soc.* **1978**, *100*, 4725.

(25) Bancroft, D. P.; Cotton, F. A.; Falvello, L. R.; Schwoltzer, W. *Inorg. Chem.* **1986**, *25*, 763.

(26) Bancroft, D. P.; Cotton, F. A.; Falvello, L. R.; Schwoltzer, W. *Inorg. Chem.* **1986**, *25*, 1015.

(27) Bancroft, D. P.; Cotton, F. A. *Inorg. Chem.* **1988**, *27*, 1633.

(28) Tylicki, R. M.; Wu, W.; Fanwick, P. E.; Walton, R. A. *Inorg. Chem.* **1995**, *35*, 988.

(29) Cayton, R. H.; Chisholm, M. H.; Putilina, E. F.; Folting, K.; Huffman, J. C.; Moodley, K. G. *Inorg. Chem.* **1992**, *31*, 2928.

(30) Mashima, K.; Nakano, H.; Nakamura, A. *J. Am. Chem. Soc.* **1993**, *115*, 11632.

(31) Cotton, F. A.; Mason, M. *J. Am. Chem. Soc.* **1965**, *87*, 921.

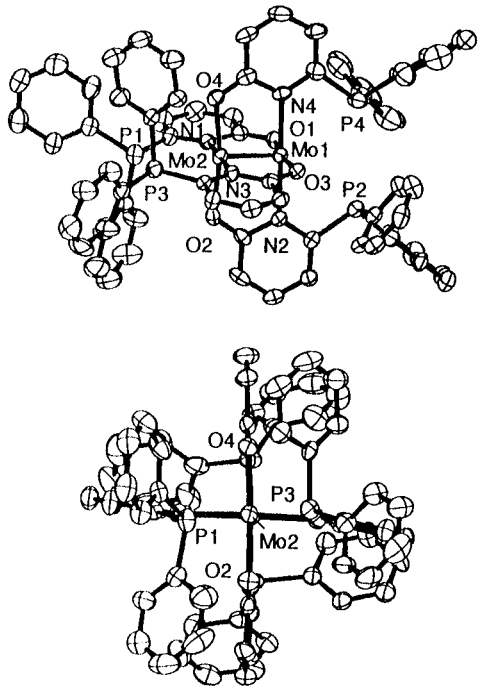

Figure 1. Two ORTEP drawings of **1**: a perspective perpendicular to the Mo−Mo vector (top) and a view down the metal−metal bond (bottom). Thermal ellipsoids are drawn at the 30% probability.

Table 1. Selected Bond Distances (Å) and Angles (deg) of $Mo_2(pyphos)_4$ (**1**)

distances	Å	angles	deg
Mo(1)−Mo(2)	2.098(2)	Mo(2)−Mo(1)−O(1)	95.9(3)
Mo(1)−O(1)	2.086(8)	Mo(2)−Mo(1)−O(3)	94.4(2)
Mo(1)−O(3)	2.075(8)	Mo(2)−Mo(1)−N(2)	89.8(3)
Mo(1)−N(2)	2.18(1)	Mo(2)−Mo(1)−N(4)	90.4(3)
Mo(1)−N(4)	2.17(1)	O(1)−Mo(1)−O(3)	169.6(4)
Mo(2)−O(2)	2.077(8)	O(1)−Mo(1)−N(2)	91.6(3)
Mo(2)−O(4)	2.071(9)	O(1)−Mo(1)−N(4)	86.9(3)
Mo(2)−N(1)	2.193(9)	O(3)−Mo(1)−N(2)	87.8(3)
Mo(2)−N(3)	2.163(9)	O(3)−Mo(1)−N(4)	93.6(3)
P(1)···P(3)[a]	3.754(6)	N(2)−Mo(1)−N(4)	178.6(3)
P(2)···P(4)[a]	3.826(5)	Mo(1)−Mo(2)−O(2)	95.7(3)
		Mo(1)−Mo(2)−O(4)	95.2(3)
		Mo(1)−Mo(2)−N(1)	89.8(3)
		Mo(1)−Mo(2)−N(3)	90.9(3)
		O(2)−Mo(2)−O(4)	169.0(4)
		O(2)−Mo(2)−N(1)	90.5(3)
		O(2)−Mo(2)−N(3)	87.1(3)
		O(4)−Mo(2)−N(1)	88.4(4)
		O(4)−Mo(2)−N(3)	93.9(3)
		N(1)−Mo(2)−N(3)	177.5(3)

[a] Nonbonded contact.

approximates closely to D_{2d} symmetry, and its structural feature is similar to that of $Mo_2(mhp)_4$ (mhp = 6-methylpyridonate).[24] The Mo−Mo distance (2.098(2) Å) of **1** is unexceptional for that of $\sigma^2\pi^4\delta^2$ quadruply-bonded Mo^{II}_2 and is comparable to that of $Mo_2(O_2CCH_3)_4$ (2.0934(8) Å)[32] and $Mo_2(mhp)_4$ (2.065(1) Å)[24] but is shorter than that of typical triply-bonded Mo^{III}_2 complexes such as $Mo_2(OCH_2CMe_3)_6$ (2.222(2) Å),[33] $Mo_2(OCHMe_2)_4(mhp)_2$ (2.206(1) Å),[34] and $Mo_2(O_2CMe)_4(CH_2CMe_3)_2$ (2.130(1) Å).[35]

(32) Cotton, F. A.; Mester, Z. C.; Webb, T. R. *Acta Crystallogr.* **1974**, *B30*, 2768.

(33) Chisholm, M. H.; Cotton, F. A.; Murillo, C. A.; Reichert, W. W. *Inorg. Chem.* **1977**, *16*, 1801.

(34) Chisholm, M. H.; Folting, K.; Huffman, J. C.; Rothwell, I. P. *Inorg. Chem.* **1981**, *20*, 2215.

(35) Chisholm, M. H.; Huffman, J. C.; Van Der Sluys, W. G. *Inorg. Chim. Acta* **1986**, *116*, L13.

Two vacant coordination sites at both axial positions of the Mo−Mo quadruple bond are sufficient to have a transition metal atom since the distances between two phosphorus atoms arranged at each mutually *trans* position are 3.826(6) Å and 3.753(6) Å. Complex **1** has an eclipsed structure with two pairs of pyridonates placed at right angles, which is an important general feature of quadruply-bonded dinuclear complexes.[16] The vector of P···N···O of pyphos ligands does not parallel with that of Mo−Mo bond, and thus dihedral angles between the plane defined by P···N−Mo and the plane defined by N−Mo−Mo in four pyphos ligands are 9°, 179°, 4°, and 179°.

Syntheses and Structures of $Mo_2Pd_2X_4(pyphos)_4$ (2) and $Mo_2Pt_2X_4(pyphos)_4$ (4) (a: X = Cl; b: X = Br; c: X = I). The dinuclear complex **1** reacted immediately with 2 equiv of $PdCl_2(PhCN)_2$ in dichloromethane to give a tetranuclear complex, $Mo_2Pd_2Cl_4(pyphos)_4$ (**2a**) (eq 6), in which two $PdCl_2$ moieties are coordinated by two sets of *trans* arranged phosphorus atoms of the pyphos ligands and thus are placed at both axial positions of Mo_2 core, but there is no direct bonding interaction between two $PdCl_2$ and Mo_2 core. The $^{31}P\{^1H\}$ NMR spectrum of **2a** displayed a singlet peak at δ 16.1, a value which is close to that (δ 17.1) of the related Pd(II) mononuclear complex, $PdCl_2(pyphosH)_2$ (**3a**).[36] A bromo derivative, $Mo_2Pd_2Br_4(pyphos)_4$ (**2b**), was also synthesized by the reaction of **1** and 2 equiv of $PdBr_2(cod)$ (cod = 1,5-cyclooctadiene). In contrast, when we measured the $^{31}P\{^1H\}$ NMR spectrum of a reaction mixture of **1** and 2 equiv of $PdI_2(cod)$ in $CDCl_3$, no signal assignable to the corresponding iodo derivative was observed. This is ascribed to the spontaneous formation of a reduced Pd−Mo bonded product, $Mo_2Pd_2I_2(pyphos)_4$ (**6c**) (*vide infra*), under this reaction condition.

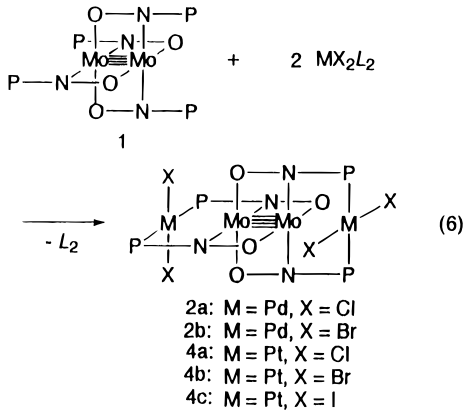

This synthetic method was applied to the synthesis of the corresponding platinum complexes. Platinum(II) complexes such as $PtCl_2(cod)$ react with **1** slower than the palladium(II) analogues. A reaction mixture of **1** and 2 equiv of $PtCl_2(cod)$ at 40 °C for 4 days resulted in the quantitative formation of a tetranuclear complex, $Mo_2Pt^{II}_2Cl_4(pyphos)_4$ (**4a**), whose structure is the same as that of **2**. The $^{31}P\{^1H\}$ NMR spectrum of **4a** displayed a singlet peak at δ 12.6 (J_{Pt-P} = 3592 Hz) due to the four equivalent phosphorus atoms coordinating to platinum(II). This chemical shift value and the Pt−P coupling constant are the same as those (δ 12.6 ppm, J_{Pt-P} = 3592 Hz) found for a mononuclear platinum(II) complex, $PtCl_2(pyphosH)_2$ (**5a**).[36] A bromo derivative, $Mo_2Pt_2Br_4(pyphos)_4$ (**4b**), and an iodo derivative, $Mo_2Pt_2I_4(pyphos)_4$ (**4c**), were synthesized similarly by reaction of **1** with 2 equiv of $PtBr_2(cod)$ and $PtI_2(cod)$, respectively, in dichloromethane. The $^{31}P\{^1H\}$ NMR spectra of **4b** (δ 11.4, J_{Pt-P} = 3534 Hz) and **4c** (δ 7.9, J_{Pt-P} = 3283

(36) Nakano, H.; Nakamura, A.; Mashima, K. *Inorg. Chem.* **1996**, *35*, 4007.

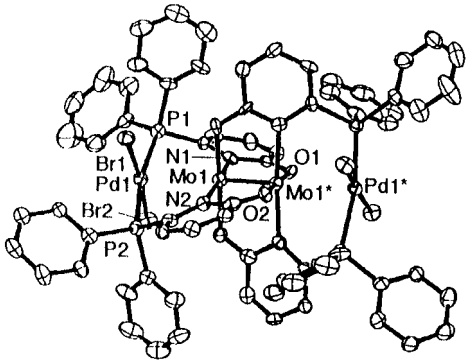

Figure 2. Molecular structure of **2b** with a labeling scheme. Thermal ellipsoids are drawn at the 30% probability.

Table 2. Selected Bond Distances (Å) and Angles (deg) of **2a**, **2b**, and **4a**[a]

	2a	**2b**	**4a**
	Distances, Å		
Mo1—Mo1*	2.096(3)	2.095(4)	2.101(2)
Mo1—M1	2.943(2)	2.902(3)	2.9292(9)
M1—X1	2.287(4)	2.427(3)	2.307(3)
M1—X2	2.282(5)	2.433(3)	2.304(3)
M1—P1	2.341(5)	2.344(7)	2.320(3)
M1—P2	2.333(6)	2.347(7)	2.323(3)
Mo1—O1	2.06(1)	2.08(2)	2.110(7)
Mo1—O2	2.10(1)	2.07(2)	2.096(7)
Mo1—N1	2.14(1)	2.12(2)	2.160(8)
Mo1—N2	2.15(1)	2.16(2)	2.152(8)
P(1)···P(2)[b]	4.638(8)	4.666(9)	4.615(5)
	Angles, deg		
M1—Mo1—Mo1*	179.2(1)	177.4(1)	179.43(5)
Mo1—M1—P1	82.8(1)	84.6(2)	83.54(7)
Mo1—M1—P2	83.0(1)	83.4(2)	83.73(7)
Mo1—M1—X1	95.0(1)	91.61(9)	94.35(8)
Mo1—M1—X2	92.4(1)	94.7(1)	93.27(8)

[a] M denotes the metal atom at the axial position of Mo—Mo, and X denotes halogen atoms bound to M; M = Pd, X = Cl for **2a**, M = Pd, X = Br for **2b**, and M = Pt, X = Cl for **4a**. [b] Nonbonded contact.

Hz) are quite similar to those of the related Pt(II) mononuclear complexes, *trans*-$PtBr_2(pyphosH)_2$ (**5b**) (δ 11.4, J_{Pt-P} = 3534 Hz) and *trans*-$PtI_2(pyphosH)_2$ (**5c**) (δ 7.9, J_{Pt-P} = 3381 Hz), respectively.[36] The ^{1}H NMR spectra of **4** are also similar to those of **5**.

The complexes **2a**, **2b**, and **4a** were crystallized in C_2/c space group. Their structural features are essentially the same, and thus the crystal structures of **2b** and **4a** are shown in Figures 2 and 3, respectively. Interatomic distances and angles of **2a**, **2b**, and **4a** are given in Table 2. In these complexes, a C_2 axis is passing through the center of two molybdenum atoms and therefore the half of them, *i.e.*, the moiety of $MoMX_2(pyphos)_2$, is a crystallographically unique part. The Pd—Mo distances of **2a** [2.943 (2) Å] and **2b** [2.902(3) Å] and the Pt—Mo distance of **4a** [2.9292 (9) Å] are too long for both atoms to interact strongly. This is consistent with the fact that the Mo—Mo distance [2.095(4)—2.101(2) Å] of **2a**, **2b**, and **4a** is almost the same as that of **1**. Both M(II) atoms are in a square-planar configuration comprised of two halogen atoms and two phosphorus atoms in *trans* arrangement. Two MX_2P_2 planes are oriented perpendicular to the vector of Mo—Mo bond. Each of the palladium and the platinum atoms is somewhat deviated outside from the position expected for a normal square coordination plane and close to tetrahedral. The coordination geometry of M(II) approaches to tetrahedron. The acute angles were observed for Mo—M—P (M = Pd for **2a** and **2b**, M = Pt for **4a**) [82.8(1)—84.6(2) degree, while the angles of Mo—M—X [91.61(9)—95.0(1)°] are obtuse. This distortion might be resulted from longer Pd···Mo distances than the distance of P—N chelation.

Syntheses of $Mo_2Pd_2X_2(pyphos)_4$ (6) and $Mo_2Pt_2X_2(pyphos)_4$ (7) (a: X = Cl; b: X = Br; c: X = I). In the presence of Et_4NBH_4, treatment of **1** with 2 equiv of $PtI_2(cod)$ for 2 days resulted in the formation of a tetranuclear complex $Mo_2Pt_2I_2(pyphos)_4$ (**7c**) in 36% yield (eq 7). Spectral data as well as elemental analysis revealed that **7c** has two Pt(I) ions,

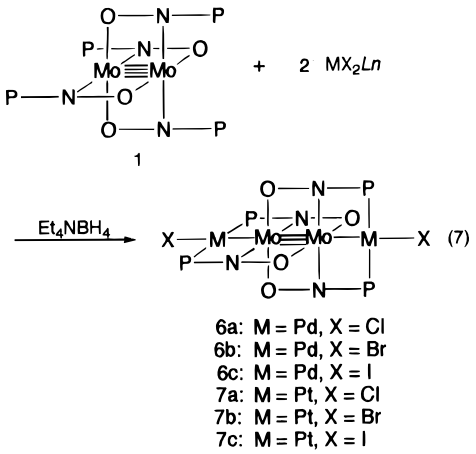

and thus two platinum ions are reduced to Pt(I) in the reaction course. The $^{31}P\{^1H\}$ NMR spectrum of **7c** in $CDCl_3$ displayed a peak at δ 26.7 (J_{Pt-P} = 3331 Hz) and was different from that of **4c**, indicating that all phosphorus atoms coordinated to platinum(I) atoms. In the ^{1}H NMR spectrum of **7c**, 3-H and 5-H resonances of the pyphos ligand are found to have an upfield shift (ca. 1.0 ppm) from those of **4c**, but 4-H resonance is displayed by downfield shift (0.6 ppm). Such a change in the chemical shift of pyridone protons upon formation of **7c** from **4c** could be due to the decrease of magnetic anisotropy around Mo_2 core.[37] During a reaction course, complex **4c** was detected by $^{31}P\{^1H\}$ NMR spectroscopy. Thus, complex **7c** was prepared alternatively by the reduction of **4c** by using Et_4NBH_4 in dichloromethane, but chemical yield was low (11%) (eq 8). The most convenient method for the preparation of **7c** is heating at 300 °C *in vacuo* of solid sample derived from **1** and 2 equiv of $PtI_2(cod)$ without any reductant (eq 8). This reaction is accompanied by an elimination of iodine (see Experimental Section). Complex **7a** and **7b** were synthesized by reaction of **1** with 2 equiv of $PtCl_2(cod)$ and $PtBr_2(cod)$, respectively. At the early stage of these reactions, **4a** and **4b** were also detected by $^{31}P\{^1H\}$ NMR spectroscopy.

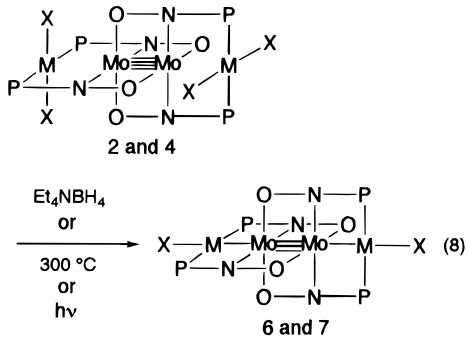

Palladium derivatives **6a**—**c** were prepared by the similar reactions (eqs 7 and 8). Treatment of **1** with 2 equiv of $PdCl_2(PhCN)_2$ in the presence of Et_4NBH_4 for 2 h led to the

(37) Cotton, F. A.; Ren, T. *J. Am. Chem. Soc.* **1992**, *114*, 2237.

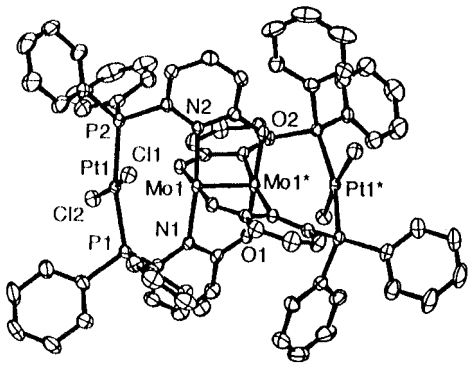

Figure 3. Molecular structure of **4a** with a labeling scheme. Thermal ellipsoids are drawn at the 30% probability.

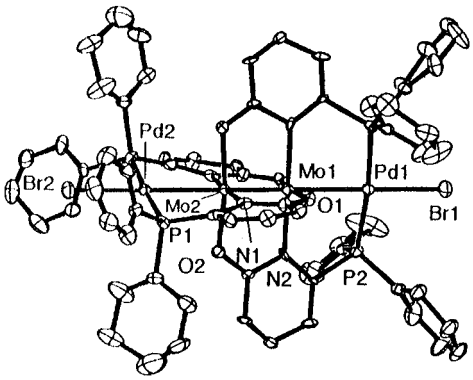

Figure 4. Molecular structure of **6b**. Thermal ellipsoids are drawn at the 30% probability.

tetranuclear complex, $Mo_2Pd_2Cl_2(pyphos)_4$ (**6a**), in 40% yield (eq 7). The formation of **6a** also proceeded stepwise since **6a** was readily prepared by the reaction of **2a** with Et_4NBH_4 in dichloromethane (60% yield) (eq 8). Complex **6b** was prepared by treatment of **1** with 2 equiv of $PdBr_2(cod)$ in the presence of Et_4NBH_4 and reduction of **2b** by Et_4NBH_4. Gentle heating up to 300 °C in attempts to determine the melting points for **2a** and **2b** did not cause melting, but the complexes were converted to the palladium(I) complexes, **6a** and **6b** (eq 8). Reaction of **1** with 2 equiv of $PdI_2(cod)$ at room temperature gave rise to $Mo_2Pd_2I_2(pyphos)_4$ (**6c**) in 50% yield without any reducing reagent since $PdI_2(cod)$ is easily reducible.

When we measured Raman spectra of **2** and **4** (*vide infra*), photochemical reduction of **2** and **4** readily proceeded, and thereby the peak of photo reduction product **6** and **7** was detected concurrently (eq 8).

Crystal Structures of 6 and 7. Crystal structure of **6a** was previously communicated.[30] The crystal structures of **6b**, **6c**, and **7** were determined by X-ray analysis, and structural feature of all **6** and **7** are described. Complexes **6** and **7** crystallized in two series of the isomorphous packing structures; one is tetragonal space group $I4_1$, and the other is monoclinic space group $P2_1/n$. Complexes **6a**, **6b**, and **7a** crystallized in $I4_1$ space group which possesses a C_2 axis in the molecule, while **6c**, **7b**, and **7c** crystallized in $P2_1/n$ without any crystallographic symmetry within the molecule.

Figure 4 shows two drawings of **6b**. The interatomic distances and bond angles of **6** and **7** are listed in Tables 3 and 4, respectively. Four metal atoms and two bromine atoms are aligned on a C_2 axis and thus the Br—Pd—Mo—Mo—Pd—Br skeleton supported by four pyphos ligands is linear. Two Pd(I) atoms occupy both axial positions of the Mo_2 moiety, and each palladium atom has the square planar geometry comprised of two phosphorus atoms in *trans* arrangement, one bromine atom and one molybdenum atom. The coordination planes of two Pd(I) atoms are coplanar to the Mo—Mo bond. The Mo—Mo bond length (2.1221(9) Å) of **6b** is longer than that found for **1**, **2a**, **2b**, and **4a**, indicating that the Mo—Mo bond is elongated by the coordination of two Pd(I) atoms. The complex **6b** has two Mo—Pd distances, *i.e.*, 2.687(4) Å and 2.690(4) Å, values which are short enough to be regarded as a single bond.

Table 3. Selected Bond Distances (Å) of **6** and **7**[a]

	6a	**6b**	**6c**
Mo1—Mo2	2.1208(9)	2.1221(9)	2.119(2)
Mo1—Pd1	2.689(4)	2.687(4)	2.711(2)
Mo2—Pd2	2.679(4)	2.690(4)	2.687(2)
Pd1—X1	2.42(1)	2.562(5)	2.695(2)
Pd2—X2	2.42(1)	2.511(4)	2.680(2)
Pd1—P2	2.283(6)	2.282(6)	2.274(6)
Pd1—P4			2.277(6)
Pd2—P1	2.287(6)	2.285(7)	2.275(6)
Pd2—P3			2.284(6)
Mo1—O1	2.04(1)	2.04(1)	2.03(1)
Mo1—O3			2.08(1)
Mo1—N2	2.15(2)	2.19(2)	2.16(2)
Mo1—N4			2.17(1)
Mo2—O2	2.05(2)	2.06(2)	2.05(1)
Mo2—O4			2.06(1)
Mo2—N1	2.25(2)	2.22(1)	2.19(2)
Mo2—N3			2.20(2)
P···P[b]	4.57(1)	4.57(1)	4.539(8)
P···P[b]	4.56(1)	4.56(1)	4.541(9)
	7a	**7b**	**7c**
Mo1—Mo2	2.134(1)	2.135(2)	2.135(2)
Mo1—Pt1	2.687(3)	2.647(1)	2.682(2)
Mo2—Pt2	2.639(4)	2.668(1)	2.669(2)
Pt1—X1	2.42(1)	2.534(2)	2.703(1)
Pt2—X2	2.44(1)	2.542(2)	2.695(2)
Pt1—P2	2.247(8)	2.253(5)	2.260(5)
Pt1—P4		2.263(5)	2.256(5)
Pt2—P1	2.284(7)	2.256(4)	2.266(6)
Pt2—P3		2.261(4)	2.258(6)
Mo1—O1	2.03(2)	2.06(1)	2.05(1)
Mo1—O3		2.07(1)	2.04(1)
Mo1—N2	2.23(2)	2.19(1)	2.16(2)
Mo1—N4		2.20(1)	2.18(1)
Mo2—O2	2.09(1)	2.07(1)	2.06(1)
Mo2—O4		2.06(1)	2.07(1)
Mo2—N1	2.18(2)	2.17(1)	2.20(1)
Mo2—N3		2.18(1)	2.22(1)
P···P[b]	4.57(1)	4.510(6)	4.508(7)
P···P[b]	4.49(2)	4.499(6)	4.512(8)

[a] X denotes halogen atoms bound to M, X = Cl for **6a** and **7a,** X = Br for **6b** and **7b**, and X = I for **6c** and **7c**. [b] Distances between two atoms arranged at a mutually *trans* position.

The chloro complex **6a** has the same arrangement with **6b**.[30] Complex **6c** crystallized in the $P2_1/n$ space group. Complex **6c** has the quite similar disposition to **6b** although the entire molecule constitutes an asymmetric unit and no crystallographic symmetry is imposed on it.

The platinum complexes **7** have essentially the same stereochemical arrangement as the palladium analogue. Complex **7c** is isomorphous with **7b** and **6c**, while complex **7a** is isomorphous with **6a** and **6b**. Figure 5 shows the drawing of **7b**. The Mo—Mo distance of **7** lies in a range of 2.134(1)−2.135(2) Å , which is longer than that of **1** and is significantly longer than those (2.119(2)−2.1221(9) Å) of palladium complexes **6**. The Pt—Mo distances (2.639(4)−2.687(3) Å) of **7** are shorter than the Pd—Mo distances (2.679(4)−2.711(2) Å) of **6**. The bonding interaction between the platinum atom and the molybdenum atom is stronger than that between the palladium atom and the molybdenum atom.

Table 4. Selected Bond Angles (deg) of **6** and **7**[a]

	6a	**6b**	**6c**
Pd1—Mo1—Mo2	180.00	180.00	179.6(1)
Pd2—Mo2—Mo1	180.00	180.00	176.4(1)
X1—Pd1—Mo1	180.00	180.00	177.9(1)
X2—Pd2—Mo2	180.00	180.00	174.83(9)
Mo2—Pd2—P1	87.5(2)	87.9(2)	86.7(1)
Mo2—Pd2—P3			88.1(1)
Mo1—Pd1—P2	87.1(2)	86.7(2)	86.1(1)
Mo1—Pd1—P4			85.5(1)
Mo2—Mo1—O1	93.8(5)	96.6(5)	94.5(3)
Mo2—Mo1—O3			94.3(3)
Mo1—Mo2—O2	97.4(5)	94.3(5)	93.6(3)
Mo1—Mo2—O4			96.3(3)
Mo1—Mo2—N1	89.0(4)	87.5(4)	88.3(4)
Mo1—Mo2—N3			89.6(4)
Mo2—Mo1—N2	88.3(4)	89.5(4)	90.0(4)
Mo2—Mo1—N4			88.8(4)
	7a	**7b**	**7c**
Pt1—Mo1—Mo2	180.00	177.03(8)	179.57(9)
Pt2—Mo2—Mo1	180.00	179.41(8)	177.51(9)
X1—Pt1—Mo1	180.00	173.61(7)	177.96(7)
X2—Pt2—Mo2	180.00	176.83(7)	174.76(6)
Mo2—Pt2—P1	88.8(2)	86.7(1)	88.7(1)
Mo2—Pt2—P3		87.4(1)	87.6(1)
Mo1—Pt1—P2	87.6(2)	88.2(1)	86.6(1)
Mo1—Pt1—P4		89.5(1)	87.1(1)
Mo2—Mo1—O1	92.5(6)	94.1(3)	93.4(3)
Mo2—Mo1—O3		93.5(3)	95.0(3)
Mo1—Mo2—O2	97.2(5)	94.0(3)	93.9(3)
Mo1—Mo2—O4		93.1(3)	93.4(3)
Mo1—Mo2—N1	91.8(6)	88.5(3)	90.1(3)
Mo1—Mo2—N3		89.5(3)	89.4(4)
Mo2—Mo1—N2	86.1(5)	89.2(3)	89.0(4)
Mo2—Mo1—N4		90.0(3)	89.4(3)

[a] X denotes halogen atoms bound to M, X = Cl for **6a** and **7a,** X = Br for **6b** and **7b**, and X = I for **6c** and **7c**.

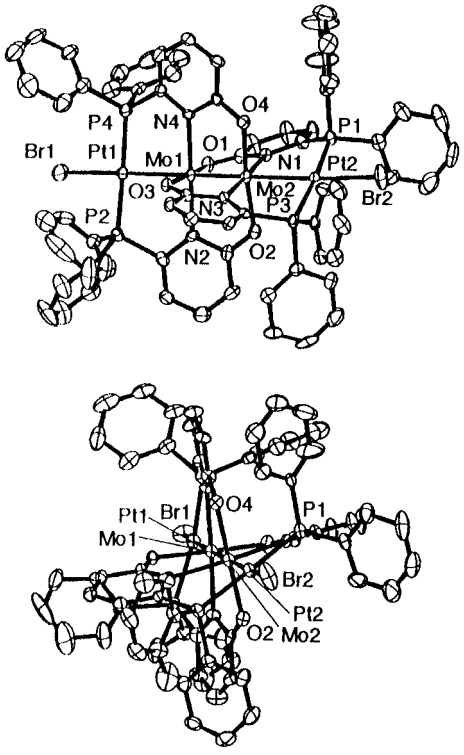

Figure 5. Two ORTEP drawings of **7b**; perspective perpendicular to the Pt—Mo—Mo—Pt vector (top) and a view down the metal−metal bond (bottom). Thermal ellipsoids are drawn at the 30% probability.

The distance of N···O chelation (2.3 Å) of pyphos ligands in **1**, **2**, **4**, **6**, and **7** is moderately longer than the Mo—Mo bond distance found for these complexes. The Mo—Mo distance (2.065(1) Å) of $Mo_2(mhp)_4$ is shorter than that of **1**, **2**, **4**, **6**, and **7**, although $Mo_2(mhp)_4$ has almost the same distance (ca. 2.3 Å) of four N···O chelations as these complexes.[24] This indicates that the Mo—Mo distance is not affected by the N···O chelation. Moreover, no significant variation is found for the P···N distances among **1**, **2**, **4**, **6**, and **7**. Thus the coordination of two M(I) atoms to both ends of the Mo_2 core in **6** and **7** elongates the Mo—Mo distance and shortens the Mo—M bond, resulting in the new addition reaction of two metals to a metal-to-metal multiple bond.

Table 5. UV−vis Absorption Maxima of **1**, **2**, **4**, **6**, and **7**

complex	λ_{max} (nm) (ϵ (M^{-1} cm^{-1}))	
1	465 (9.0×10^3)	
2a	482 (3.2×10^3)	
2b	486 (2.5×10^3)	
4a	485 (4.6×10^3)	
4b	515 (4.3×10^3)	
4c	504 (*a*)	
6a	458 (1.3×10^4)	642 (3.0×10^4)
6b	470 (1.3×10^4)	662 (4.7×10^4)
6c	489 (5.3×10^3)	706 (4.0×10^4)
7a	409 (1.4×10^4)	506 (3.1×10^4)
7b	414 (1.4×10^4)	523 (4.7×10^4)
7c	418 (1.6×10^4)	564 (7.4×10^4)

[a] Contamination of complex **7c**.

Dihedral angles between the planes defined by P···N—Mo and the planes defined by N—Mo—Mo indicate the degree of the deviation of pyphos ligands from the line of Mo—Mo. The dihedral angles of **2** and **4** are around 21°, and the averaged dihedral angles of **6** and **7** lie in the range 12 and 16°. All these values are larger than those of **1**, indicating that the direction of diphenylphosphino moiety of pyphos ligand in **2**, **4**, **6**, and **7** turned aside from that observed for **1**. This divergence might be ascribed to the insertion of M atoms between the each *trans* phosphorus atoms. This insertion of M atoms between two phosphorus atoms makes the P···P distances (ca. 4.5−4.6 Å) in **2**, **4**, **6**, and **7** considerably longer than those in **1** (3.8 Å). In spite of the observed deviation of pyphos ligands from the original position, the linearity of the M—Mo—Mo—M fragment is maintained. Thus the pyphos ligand has a remarkable ability to align metal atoms linear.

Electronic Spectra. The spectral data of **1**, **2**, **4**, **6**, and **7** are numerically shown in Table 5. The dinuclear complex **1** exhibited one distinct peak at 465 nm, which is typical of $\delta-\delta^*$ excitation due to the Mo—Mo quadruple bond.[38,39] Each electronic spectrum of **2** and **4** showed one distinct peak at 482−486 and 485−515 nm, respectively, indicating that these have the quadruply bonded Mo—Mo bond.

In the reaction course of formation of the linear tetranuclear complexes **6** and **7**, the color of the solution changed from red to green (M = Pd) or to purple (M = Pt). The tetranuclear complexes **6** and **7** show two characteristic visible absorption maxima, both of which serve as a sensitive probe for Mo—M (M = Pd, Pt) and Mo—Mo bonding. The peak at the higher energy is assignable to $\delta-\delta^*$ excitation of the Mo—Mo bond. The other absorption of **6** and **7** is observed in the ranges of 506−564 and 642−706 nm, respectively, while **1**, **2**, and **4** have no peak in these regions. Accordingly, the latter peak is ascribed to the excitation at Mo—M bond, *i.e.*, essentially charge transfer from Mo atom to M atom.

The position of MMCT band observed for **6** and **7** is in accordance with the spectrochemical series of halo ligands, I

(38) Martin, D. S.; Newman, R. A.; Fanwick, P. E. *Inorg. Chem.* **1979**, *18*, 2511.
(39) Martin, D. S.; Huang, H.-W. *Inorg. Chem.* **1990**, *29*, 3674.

Table 6. Selected Raman Frequencies of **1**, **2**, **4**, **6**, and **7**

complex	ν(Mo—Mo) (cm^{-1})	others (cm^{-1})		d(Mo—Mo) (Å)[a]
1	394			2.098(2)
2a	403			2.096(3)
2b	403			2.095(4)
4a	403			2.101(2)
4b	395			
4c	395			
6a	386	122	84	2.1208(9)
6b	386	122	82	2.1221(9)
6c	387	116	73	2.119(2)
7a	381	126	81	2.134(1)
7b	382	127	81	2.135(2)
7c	381	120	73	2.135(2)

[a] Distance of Mo—Mo multiple bond.

< Br < Cl, depending on electronegativities of halogen atoms. Both complexes **6** and **7** have the same tendency, *i.e.*, the differences between **a** (X = Cl) and **b** (X = Br) are smaller than those between **b** (X = Br) and **c** (X = I). On the comparison of CT band between **6** and **7** with the same halo ligand set, **6** have 140 nm longer wavelength than **7**. The maxima of $\delta-\delta^*$ excitation are also in accordance with the spectrochemical series of halogen atoms. Comparing the influence of M atoms to $\delta-\delta^*$ of Mo—Mo, the excitation in **7** requires higher energy than that of **6**. The differences of peak wavelengths between **6a** and **6b** and between **6b** and **6c** are 12 and 19 nm, respectively, while those for **7** equal 5 nm. These indicate that the Mo—Mo multiple bonding of **6** is more delicately influenced by the halogen ligands than that of **7**.

Raman Spectra. The Raman active ν(Mo—Mo) mode has provided a highly useful spectroscopic probe of the nature of bonding in many of the dimolybdenum complexes.[40,41] The wavenumbers of ν(Mo—Mo) together with the Mo—Mo distance for **1**, **2**, **4**, **6**, and **7** are listed in Table 6. Complex **1** has a ν(Mo—Mo) peak at 394 cm^{-1} which is consistent with the frequency of ν(Mo—Mo) observed for $Mo_2(mhp)_4$[24] and $Mo_2(O_2CCH_3)_4$.[42−45] The ν(Mo—Mo) of **2** and **4** is observed at slightly higher frequency (395−403 cm^{-1}) than that of **1**. This is consistent with the crystallographic result that the Mo—Mo bond distance of **2** and **4** is almost the same as that of **1**. The effects of halo ligands of **2** were too small to be detected, and all three complexes **2** have the same value (403 cm^{-1}) of ν(Mo—Mo). As mentioned above, photochemical reduction of **2** and **4** proceeded. Figure 6 shows time-dependent spectra of **2b** upon irradiation of 514.5 nm laser. The intensity of ν(Mo—Mo) (386 cm^{-1}) of **6b** increased at the expense of the intensity of that (403 cm^{-1}) of **2b**. For platinum complexes **4**, the ν(Mo—Mo) peak was observed at the range of 395−403 cm^{-1} accompanied with the signal of each reduction product of **7**, whose intensity increased with irradiation time.

The resonance Raman spectra were measured for **6** and **7**. The most probable frequency assignable to ν(Mo—Mo) in **6** and **7** was observed at 381−387 cm^{-1}, lower wavenumber than those in **1**, **2**, and **4**. The assignment of this peak is strongly supported by the excitation profiles of resonance Raman spectra. The example of **6c** is shown in Figure 7, in which eight

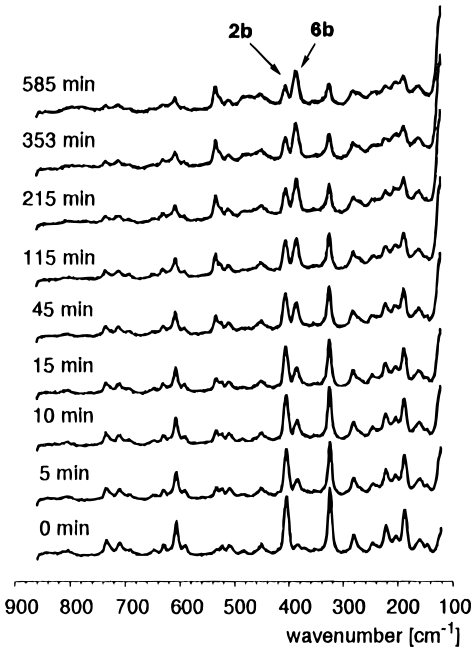

Figure 6. Photoreduction process of **2b** with 514.5 nm laser irradiation monitored by Raman spectra at moderate time intervals.

Scheme 1

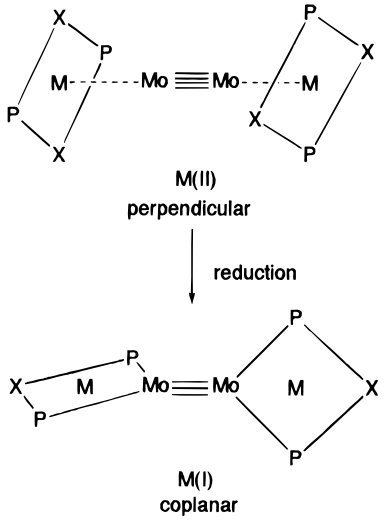

wavelengths of excitation were used. The excitation profiles of these spectra are shown in Figure 8. The most effective enhancement of the ν(Mo—Mo) peak strength was observed with the excitation of 454.5 nm. The spectrum with longer wavelength of laser excitation gave the ν(Mo—Mo) peak with lower intensity, and the peak excited by 632.8 nm laser line had the lowest peak intensity. This is attributed to the closest wavelength of excitation (454.5 nm) to the absorption at 416 nm. On the other hand, two peaks at 116 and 73 cm^{-1} are enhanced by the excitation whose wavenumber was the closest to the longer wavelength absorption maximum at 706 nm.

A similar situation was observed for five other complexes of **6a**, **6b**, and **7a**−**c**. The resonance Raman spectra of these complexes were measured with three wavelengths (457.9, 514.5, and 632.8 nm) of laser excitation. In the spectra of these complexes, the most effective enhancement of the ν(Mo—Mo) peak strength was generally observed when the laser excitation of 457.9 nm was used since this excitation has the closest wavelength to the $\delta-\delta^*$ absorption around 400−500 nm. The 514.5 nm excitation gave the ν(Mo—Mo) peak with lower intensity and the peak excited by 632.8 nm laser line had the

(40) Clark, R. J. H.; Franks, M. L. *J. Am. Chem. Soc.* **1975**, *97*, 2691.
(41) Manning, M. C.; Holland, G. F.; Ellis, D. E.; Trogler, W. C. *J. Phys. Chem* **1983**, *87*, 3093.
(42) Bratton, W. K.; Cotton, F. A.; Debeau, M.; Walton, R. A. *J. Coord. Chem.* **1971**, *1*, 121.
(43) San Filippo, J. J.; Sniadoch, H. J. *Inorg. Chem.* **1973**, *12*, 2326.
(44) Ketteringham, A. P.; Oldham, C. *J. Chem. Soc., Dalton Trans.* **1973**, 1067.
(45) Clark, R. J. H.; Hempleman, A. J.; Kurmoo, M. *J. Chem. Soc., Dalton Trans.* **1988**, 973.

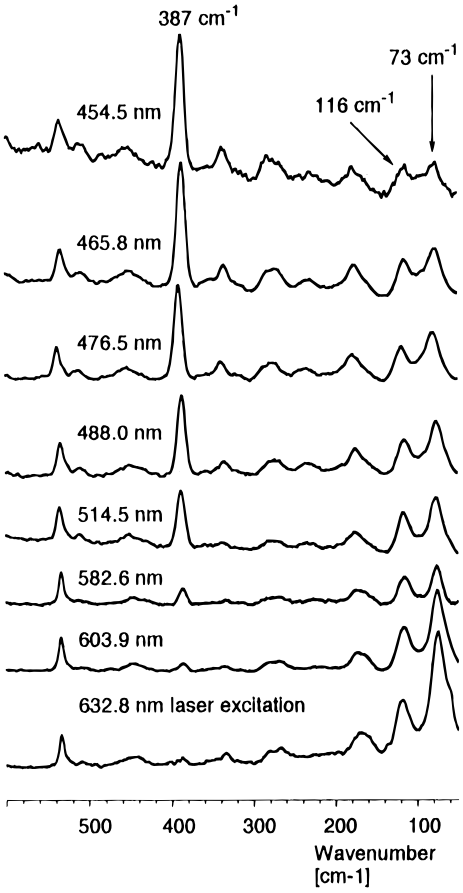

Figure 7. Resonance Raman spectra of **6c** using various wavelengths of laser excitation.

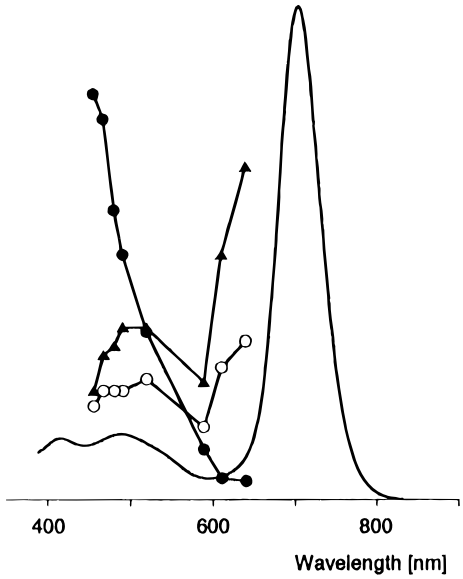

Figure 8. UV−vis spectrum and excitation profiles of **6c**. Relative intensity of peaks at 387 cm^{-1} for ●, at 116 cm^{-1} for ○, and at 73 cm^{-1} for ▲.

lowest peak intensity, while two peaks at 120−126 and 73−84 cm^{-1} are enhanced by the excitation whose wavenumber was the closest to the CT band, *i.e.*, 632.8 nm laser excitation for **6a** and **6b**, 514.5 nm for **7a**−**7f**.

Analyzing with linearly linked four atoms model, M−Mo−Mo−M, which is assumed to be in $D_{\infty h}$ point group, five of the symmetry coordinates exist.[46,47] The Raman active vibration results from three modes of Σ_g^+, Σ_g^+, and Π_g, which are described approximately by Mo−Mo stretching, M−Mo stretching and Mo−Mo−M bending, respectively. As shown in Figure 7, two Raman peaks (116 and 73 cm^{-1}) of **6c** are enhanced by the irradiation whose wavelength is close to the absorption maximum of MoM charge transfer band. Thus these peaks are ascribed to the vibrations related M−Mo bonding; however, the strict assignment is difficult at present.

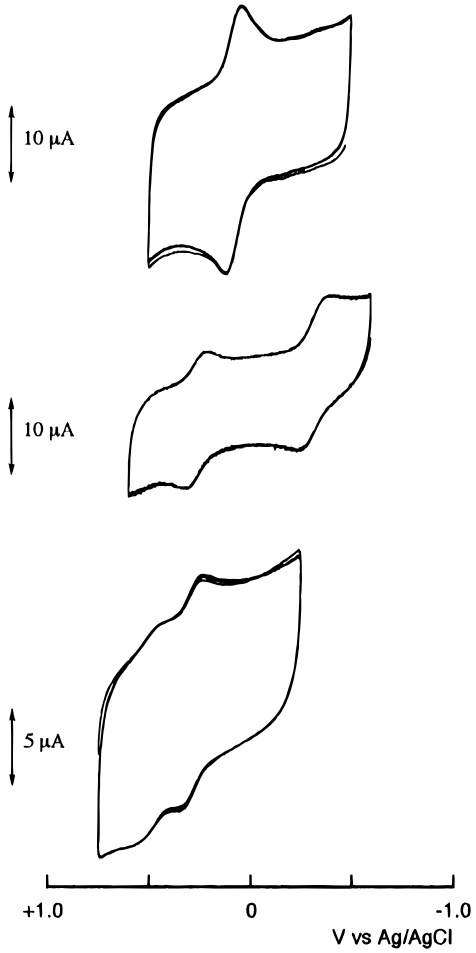

Figure 9. Cyclic voltammograms of **1** (top), **4a** (middle), and **7c** (bottom). Condition: 1.0 mM dichloromethane solution, 0.2 M tetra-*n*-butylammonium perchlorate as supporting electrode, Ag/AgCl, the scan rate of 100 mV/s.

Electrochemistry. Cyclic voltammetry of each complex is performed in dichloromethane solution containing tetra-*n*-butylammonium perchlorate as supporting electrode and data were referred to Ag/AgCl. The dinuclear complex **1** displayed a quasi-reversible redox wave at $E_{1/2} = +80$ mV (Figure 9) assignable to one-electron oxidation at the filled δ-bonding level of the Mo−Mo quadruple bond.[48−52] Cyclic voltammetry of complexes **2a**−**c**, **4b**, and **4c** gave rather complicated waves, which could not be assigned; however, the CV of complex **4a** afforded two quasi-reversible waves at $E_{1/2} = +270$ mV and

(46) Durig, J. G.; Lau, K. K.; Nagarajan, G. N.; Walker, M. J. B. *J. Chem. Phys.* **1969**, *50*, 2130.
(47) Stein, P.; Dickson, M. K.; Max Roundhill, D. *J. Am. Chem. Soc.* **1983**, *105*, 3489.
(48) Cotton, F. A.; Pedersen, E. *Inorg. Chem.* **1975**, *14*, 399.
(49) Zeitlow, T. C.; Klendworth, D. D.; Nimry, T.; Salmon, D. J.; Walton, R. A. *Inorg. Chem.* **1981**, *20*, 947.
(50) Santure, D. J.; Huffman, J. C.; Sattelberger, A. P. *Inorg. Chem.* **1985**, *24*, 371.
(51) Chisholm, M. H.; Clark, D. L.; Huffman, J. C.; Van Der Sluys, W. G.; Kober, E. M.; Lichtenberger, D. L.; Bursten, B. E. *J. Am. Chem. Soc.* **1987**, *109*, 6796.
(52) Lin, C.; Protasiewicz, J. D.; Smith, E. T.; Ren, T. *J. Chem. Soc., Chem. Commun.* **1995**, 2257.

Table 7. $E_{1/2}$ [mV] Values for **6** and **7** by Cyclic Voltammogram[a]

complex	$E_{1/2}$ [mV]	complex	$E_{1/2}$ [mV]
6a	+530, +350	**7a**	+490, +270
6b	+560, +360	**7b**	+510, +290
6c	+520, +350	**7c**	+510, +290

[a] All compounds were studied as 1.0 mM solutions in dichloromethane containing 0.2 M tetra-*n*-butylammonium perchlorate as supporting electrode at the scan rate of 100 mV/s.

−330 mV (Figure 9). The first process is the same as **1**, and the second one is attributed to a reduction process for generating **7a**.

In contrast, the tetranuclear complexes **6** and **7** display two quasi-reversible redox waves, and the electrochemical data are summarized in Table 7. Figure 9 shows representative cyclic voltammograms of **7c**. These $E_{1/2}$ values indicate that the substitution of palladium atoms with platinum atoms provides redox waves with ca. 50 mV negative shift, which is reasonable on taking account of the $M^+ \rightarrow M^{2+}$ ionization energies (Pd: 1875 kJ/mol; Pt: 1791 kJ/mol). The variation of halo ligands bound to metals hardly influences the redox process.

We examined the electrooxidation of **7c** at the sufficiently higher potential than that of the second oxidation process (+0.51 V) by using a platinum disk electrode. The electrolysis of **7c** at +0.70 V for 10 min afforded the corresponding platinum(II) complex **4c** in ca. 70% yield (monitored by $^{31}P\{^1H\}$ NMR spectrum together with electronic spectrum). The formation of **4c** may indicate that each of the two redox processes of **6** and **7** in cyclic voltammetry is a one electron oxidation process.

This assignment is supported by the following experimental results to some extent. At the potential between the first redox (+0.29 V) and that of the second redox (+0.51 V), the electrolysis of **7c** in dichloromethane was carried out. After the electrolysis at +0.45 V for 1 h was performed, the UV−vis spectrum of the electrolysis solution did not indicate distinct change, and its $^{31}P\{^1H\}$NMR spectrum displayed a sharp singlet at δ 25.6 due to the starting complex of **7c**. When **7c** was electrolyzed at +0.50 V, no change was observed in UV−vis spectrum, however, the $^{31}P\{^1H\}$NMR spectrum displayed a broad signal centered at δ 25.6 with the peak width at half height of 31.8 Hz on a 109 MHz spectrometer. These results would indicate that a paramagnetic species was formed by one electron oxidation, and the resulting paramagnetic species broadened the $^{31}P\{^1H\}$NMR signal. Unfortunately, all attempts to isolate and perceive the paramagnetic species have been unsuccessful due to its rapid conversion to **7c** and unidentified materials.

Discussion

Formation of Multiply Bonded M—Mo—Mo—M Systems. The *trans*-arrangement of each two phosphorus atoms in the $Mo_2(pyphos)_4$ skeleton has superior ability to bind two other metal atoms, which are allowed to interact with the terminals of the Mo—Mo quadruple bond. The distances between each *trans* phosphorus atoms are sufficiently long to have platinum ions or palladium ions at each site.

As shown in Figures 2 and 3, the complexes **2** and **4** have two square planes comprised of M (M = Pd, Pt), two halogen atoms, and two phosphorus atoms. These planes are perpendicular to the Mo—Mo axis. The Mo—Mo bond distance indicates that they have quadruple as just found for **1**. The Raman spectra also suggested that **2** and **4** have the Mo—Mo quadruple bond based on the values of the ν(Mo—Mo) peak. Thus two M(II) atoms of **2** and **4** interact only weakly with the molybdenum atoms. The comparable situation has already been found in the dimer of trinuclear complexes such as $[Mo_2PdCl_2(pyphos)_2(O_2CCH_3)_2]_2$ (**9**)[30] and $[Mo_2PtX_2(pyphos)_2(O_2CR)_2]_2$ [R = CH_3 (**10**), R = CMe_3 (**11**)][36] in which M(II) (M = Pd, Pt) atoms are square-planar and are coordinated by two phosphorus atoms and two halogen atoms in *cis*-fashion. The M—Mo distances of **9** and **10** is comparable to those of **2** and **4** and longer than those of **6** and **7**.

The key step of the formation of **6** and **7** is the reduction of two M(II) atoms in **2** and **4**, resulting in the elimination of two halo ligands and the coordination of a Mo atom of Mo_2 core to each M(I) atom. The molybdenum atom is formally acting as a ligand of square-planar M(I) ions. The most interesting feature of this reaction is that the orientation of two coordination planes of M atoms has changed from perpendicular to coplanar to the Mo—Mo line, which is schematically shown in Scheme 1. The complexes **2** and **4** are also easily reduced by heating or photoirradiation. The platinum derivatives, **4a**−**c** are somewhat more stable than the corresponding palladium complexes, and thus the reduction of **4** takes longer times than that of **2**. Thus, it is generally concluded that the initially formed **2** and **4** are reduced to **6** and **7**, respectively. The odd oxidation state of group 10 metal atoms, *i.e.*, +1 and +3, are generally important to generate metal−metal bond and thus the reduction or oxidation is accompanied by the formation of M—M bond. Some multimetal complexes without any metal-to-metal bond were oxidized to give the metal−metal bonded ones. Representative examples are the Pt_2Pd complexes such as *cis*-$[(NH_3)_2Pt(1\text{-}MeU)_2Pd(1\text{-}MeU)_2Pt(NH_3)_2]^{2+}$ (MeU = 1-methyluracilato)[10b] and Pt_2 complexes such as $[Pt_2H(\mu\text{-dppm})_2(\eta^1\text{-dppm})]Cl$,[53] $[Pt_2Cl_2(pyt)_4]$ (pyt = anion of pyridine-2-thiol),[54] and $[Pt(C_8doH)_2Cl_2]_2$ (C_8doH represents C_8 carbocyclic α-dioximate ligand $\{C_8H_{12}(=NO)_2H\}^-$).[55]

It has been conceived that the construction of the straight linear tetrametal system including a metal−metal multiple bond is difficult. Chisholm and co-workers found that a tetranuclear complex bearing two quadruply-bonded Mo_2 moieties, $[Mo_2(O_2C\text{-}^tBu)_3]_2(\mu\text{-}2,7\text{-}O_2N_2C_8H_4)$ (**8**),[5,56] has no direct metal-to-metal interaction between two units of Mo$\overset{4}{—}$Mo which are aligned parallel. In complex **8**, each internal molybdenum atom is coordinated by the oxygen atom of its neighboring μ-carboxylates at the axial position of the Mo$\overset{4}{—}$Mo core. The oxygen bridged Mo_2O_2 geometry results in no direct bonding interaction between Mo atoms and the slip of two Mo_2 moieties out of the straight line. Such a Mo···O interaction prevents the straight linear alignment of four metals from two M_2 core in dinuclear $M_2(O_2CR)_4$ complexes[32,39,57,58] as well as in the dimer of the trinuclear complexes such as **9**,[30] **10**,[36] and **11**.[36]

Bonding Considerations. The Mo—Mo bond of **6** and **7** may be considered as formally $\pi^4\delta^2$ triple bond and is related to the $\pi^4\delta^2$ Mo—Mo triple bond of $Mo_2(O_2CMe)_4(CH_2CMe_3)_2$ (**12**),[35] where the Mo—Mo distance [2.130(1) Å] is quite close to that found for **6** and **7**. The σ-bonding interaction between two M(I) atoms and the Mo_2 moiety in **6** and **7** elongates the Mo—Mo bond by 0.02−0.03 Å from that of **1**, **2a**, **2b**, and **4a**. The Mo—Mo bond length of **6** and **7** is shorter than that of the Mo—Mo triple bond in $Mo_2(OCH_2CMe_3)_4(MeCOCHCOMe)_2$ [2.237(1) Å] and is much shorter than that of the triple bond

(53) Umakoshi, K.; Kinoshita, I.; Ichimura, A.; Ooi, S. *Inorg. Chem.* **1987**, *26*, 3551.
(54) Krevor, J. V. Z.; Yee, L. *Inorg. Chem.* **1990**, *29*, 4305.
(55) Baxter, L. A. M.; Heath, G. A.; Raptis, R. G.; Willis, A. C. *J. Am. Chem. Soc.* **1992**, *114*, 6499.
(56) Cayton, R. H.; Chisholm, M. H.; Putilina, E. F.; Folting, K. *Polyhedron* **1993**, *12*, 2627.
(57) Cotton, F. A.; Extine, M.; Gage, L. D. *Inorg. Chem.* **1978**, *17*, 172.
(58) Robbins, G. A.; Martin, D. S. *Inorg. Chem.* **1984**, *23*, 2086.

found for $Mo_2(OCH_2CMe_3)_4(MeCOCHCOMe)_2(CNCMe_3)_2$ [2.508(2) Å].[59−61]

The interaction between molybdenum and M(I) (M = Pd, Pt) is a novel aspect of our complexes. Some examples of dinuclear complexes containing the Pd−Mo single bond have been reported, *e.g.*, $[(^t\text{-BuNC})(OC)_3Mo(\mu\text{-dpm})_2PdI]^+$ (dpm = bis(diphenylphosphino)methane)[62] and $(CO)_4Mo(\mu\text{-}PCy_2)_2Pd(PPh_3)$.[63] These Pd−Mo distances (2.870(2) and 2.760(1) Å, respectively) are longer than that of **6**. Compared with the reported Mo(0)−Pt(II) bond distance of $(OC)_4Mo(\mu\text{-}PPh_2)_2Pt(PEt_3)$, 2.766(1) Å,[64] the corresponding values of **7** are shorter by 0.1 Å.

The X-ray analysis clearly shows that the Pt−Cl distances of **7a** are longer than those in **4a** and are comparable to that of $[Pt_2(\mu\text{-dppm})_2Cl(PPh_3)](PF_6)$ [2.403(14) Å].[65] Generally, M−X bonds of **6** and **7** are longer than those of the corresponding complexes **2** and **4** as well as those of the conventional M−X covalent bonds. This elongation might be explained in term of the *trans* influence of the Mo−Pt bond to the Pt−Cl one. For the metal−metal single bond, similar *trans* influence of metal−metal bond was reported in dinuclear platinum(I) complexes, $K_4[Pt_2(P_2O_5H_2)_4L_2]$ (L = SCN, NO_2, and so on),[66] and $[Pt_2(\mu\text{-dppm})_2Cl(PPh_3)](PF_6)$,[65] in which the Pt−Cl bond length [2.403(14)Å] *trans* to Pt−Pt bond is close to that of **7a**.

It is interesting to compare the influence of a halo ligand in a series of complexes **6** and **7**. The inductive effects exerted by the halo ligand are evaluated by the comparison of the bond lengths in **6** and **7**. Structural data of **6** and **7** indicate that the Mo−Mo distance is insensitive to the identity of halogen, while the mean value of the M−Mo distances is affected by changing halogen atoms, *i.e.*, **6a** (2.684 Å) ≈ **6b** (2.685 Å) < **6c** (2.699 Å) in Mo_2Pd_2 complexes and **7a** (2.662 Å) ≈ **7b** (2.658 Å) < **7c** (2.676 Å) in Mo_2Pt_2 complexes.

In contrast to the small effect by halo ligands bound to a M(I) ion, we found distinct influence of axial metal substitution to the Mo−Mo bond length. The Mo−Mo distances in Mo_2Pd_2 complexes, **6a**−**c** [2.119(2)−2.127(2) Å], are shorter by 0.01 Å than those of Mo_2Pt_2 complexes, **7a**−**c** (2.134(1)−2.135(2) Å). Compared with the M−Mo distances of **6a**−**c** with those in **7a**−**c**, the former distances are ca. 0.02 Å longer than the latter ones, nonetheless the ionic radii of both metals are almost the same. These indicate that the M−Mo bonds for M = Pt are stronger than those for M = Pd. Stronger Mo−Pt interaction might be attributed to the relativistic effect for 5d metals. Thus, it is concluded that the Mo−Mo and Mo−M (M = Pd, Pt) bond lengths are inversely related, *i.e.*, the longer Mo−Mo distance of **7** is attended by the shorter M−Mo distances. This is comparable to the relation between Cr−Cr and Cr−L (L = axial ligands) distances reported for $Cr_2(O_2CR)_4$ by Cotton *et al.*[67] It is also found that the Mo−Mo bond is only slightly extended by the axial coordination of organic ligands.[57]

Table 8. Torsion Angles of O−Mo−Mo−O for **1**, **2a**, **2b**, **4a**, **6**, and **7**

complex	O−Mo−Mo−N (deg)			
1	1.2(4)	0.1(3)	−0.5(3)	−0.2(3)
2a	11.0(5)	11.8(5)		
2b	−12.4(7)	−9.9(6)		
4a	12.1(3)	11.3(3)		
6a	4.6(6)	−1.8(6)		
6b	−2.6(6)	3.1(6)		
6c	10.0(6)	10.1(5)	9.3(5)	10.4(6)
7a	4.8(7)	−1.9(6)		
7b	10.6(4)	11.5(4)	10.3(4)	8.9(4)
7c	9.6(5)	9.8(6)	11.5(5)	10.5(5)

The torsion angle of O−Mo−Mo−N provides information to the strength of the δ bond in the Mo_2 core. The torsion angles for all complexes are listed in Table 8. The torsion angles (0.1(3)−1.2(4)°) of **1** are nearly zero, indicating that **1** has the eclipsed geometry around Mo_2 core and the maximum of the δ-bonding interaction. When two M(II) ions are introduced, the torsion angles of complexes **2a**, **2b**, and **4a** are deviated by ca. 10 degree from the desired eclipsed geometry. In complexes **6** and **7**, the iodo complexes **6c** and **7c** are deformed by 10 degree, while the torsion angles of chloro ones, **6a** and **7a**, are small. Thus, the presence of metal atoms at both axial positions of the Mo_2 core might affect slightly the $\delta-\delta^*$ overlapping. As this influence is not severe, these complexes have a considerable amount of the δ bonding on the Mo_2 core.

Conclusion

The tetranuclear complexes of **2**, **4**, **6,** and **7** are the first example of dinuclear multiply bonded molybdenum(II) complexes having later transition metal atoms as the axial ligands. The linearity of M−Mo−Mo−M (M = Pd, Pt) moieties is enforced by the $Mo_2(pyphos)_4$ skeleton. We have elucidated by single crystal X-ray analyses that **6** and **7** have the novel structure possessing four metal atoms aligned straight linearly and bonded directly each other, while there is essentially no bonding interaction between Mo(II) and M(II) in complexes **2** and **4**. The complexes **6** and **7** formally have two single M(I)−Mo(II) bonds and one triple Mo−Mo bond ($\pi^4\delta^2$). The chemical reduction of **2** and **4** readily gives **6** and **7**, respectively. Thus, the reduction is essential to the formation of the M−Mo bond. The electrochemical study indicates that all the atoms in the M−Mo−Mo−M system are electronically strongly coupled to allow two well distinguished one electron redox processes. In the $Mo_2M_2X_2(pyphos)_4$ system, the absorption maxima are tunable by substitution of M atoms and X atoms. The tetrametal skeleton of **6** and **7** is thermally and photochemically very stable and not easily collapsed, and thus this unit provides a unique part for constructing low dimensional materials, which is of our current interest.

Experimental Section

General Methods. All manipulations for air- and moisture-sensitive compounds were carried out by the use of the standard Schlenk techniques under argon atmosphere. Each solvent was purified by distillation under argon after drying over the desiccant shown below: dichloromethane, calcium hydride or phosphorus pentaoxide; diethyl ether, sodium benzophenone ketyl; chloroform-*d*, phosphorus pentaoxide; benzene-d_6, sodium/potassium alloy. $PdCl_2(PhCN)_2$,[68a] $PdX_2(cod)$

(59) Chisholm, M. H.; Folting, K.; Huffman, J. C.; Ratermann, A. L. *Inorg. Chem.* **1984**, *23*, 613.
(60) Chisholm, M. H.; Corning, J. F.; Folting, K.; Huffman, J. C.; Ratermann, A. L.; Rothwell, I. P.; Streib, W. E. *Inorg. Chem.* **1984**, *23*, 1037.
(61) Chisholm, M. H. *Angew. Chem., Int. Ed. Engl.* **1986**, *25*, 21.
(62) Balch, A. L.; Noll, B. C.; Olmstead, M. M.; Toronto, D. V. *Inorg. Chem.* **1993**, *32*, 3613.
(63) Loeb, S. J.; Taylor, H. A.; Gelmini, L.; Stephan, D. W. *Inorg. Chem.* **1986**, *25*, 1977.
(64) Powell, J.; Couture, C.; Gregg, M. R.; Sawyer, J. F. *Inorg. Chem.* **1989**, *28*, 3437.
(65) Blau, R. J.; Espenson, J. M.; Kim, S.; Jacobson, R. A. *Inorg. Chem.* **1986**, *25*, 757.
(66) Che, C.-M.; Lee, W.-M.; Mak, T. C. W.; Gray, H. B. *J. Am. Chem. Soc.* **1986**, *108*, 4446.
(67) (a) Cotton, F. A.; Extine, M. W.; Rice, G. W. *Inorg. Chem.* **1978**, *17*, 176. (b) Cotton, F. A.; Wang, W. *Nouv. J. Chim.* **1984**, *8*, 331.

Table 9. Crystallographic Data of **1**, **2**, and **4**[a,b]

complex	**1**	**2a**
formula	$C_{69}H_{54}O_4N_4P_4Mo_2Cl_2$	$C_{74}H_{64}O_4N_4P_4Mo_2Pd_2Cl_{16}$
solvent molecules	dichloromethane (one)	dichloromethane (six)
fw	1389.89	2169.17
cryst system	monoclinic	monoclinic
space group	$P2_1/c$	$C2/c$
a, Å	14.755 (9)	24.262(4)
b, Å	24.96(1)	12.300(3)
c, Å	19.58(1)	31.521(6)
β, deg	111.56(4)	112.86(1)
V, Å^3	6709 (9)	8667(3)
Z	4	4
*D*calc, g cm^{-3}	1.376	1.662
radiation	MoKα	MoKα
temp, K	296	296
linear abs coeff, cm^{-1}	5.86	13.05
cryst. size, mm	0.3 × 0.4 × 0.5	0.1 × 0.3 × 0.5
GOF	2.38	2.97
no. of unique data	12540	11716
no. of data with $I > 3\sigma(I)$	5308	3468
no. of variables	920	496
R	0.062	0.084
R_w	0.082	0.064

complex	**2b**	**4a**
formula	$C_{71}H_{58}O_4N_4P_4Mo_2Pd_2Br_4Cl_6$	$C_{72}H_{60}O_4N_4P_4Mo_2Pt_2Cl_{12}$
solvent molecules	dichloromethane (three)	dichloromethane (four)
fw	2092.17	2176.68
cryst system	monoclinic	monoclinic
space group	$C2/c$	$C2/c$
a, Å	32.540(5)	24.273(2)
b, Å	12.461(4)	12.278(3)
c, Å	19.759(3)	31.545(6)
β, deg	104.25(1)	112.87(1)
V, Å^3	7765(2)	8662(2)
Z	4	4
*D*calc, g cm^{-3}	1.789	1.669
radiation	MoKα	MoKα
temp, K	296	296
linear abs coeff, cm^{-1}	31.73	39.78
cryst. size, mm	0.1 × 0.1 × 0.5	0.3 × 0.5 × 0.7
GOF	2.85	2.73
no. of unique data	7621	13159
no. of data with $I > 3\sigma(I)$	2556	8292
no. of variables	446	452
R	0.068	0.054
R_w	0.058	0.090

[a] $R = \sum||F_o| - |F_c||/|F_o|$. [b] $R_w = [\sum w(|F_o| - |F_c|)^2/\sum wF_o^2]^{1/2}$. $w = 1/\sigma^2(F_o)$; function minimized: $\sum w(|F_o| - |F_c|)^2$.

(X = Br, I),[68b] PtX_2(cod) (X = Cl, Br, I),[68c] and 6-diphenylphosphino-2-pyridone (pyphosH)[69] were prepared according to the literature.

Physical Measurements. Nuclear magnetic resonance (^{1}H, ^{31}P NMR) spectra were measured on a JEOL JNM-GSX-270 spectrometer. All ^{1}H NMR chemical shifts were reported in ppm relative to proton impurity resonance in chloroform-*d* at δ 7.27 and benzene-d_6 at δ 7.20. The ^{31}P NMR chemical shifts were reported in ppm relative to external reference of 85% H_3PO_4 at δ 0.00. Mass spectra were recorded on a JEOL SX-102 spectrometer. Raman spectra were recorded at 298 K on a Jasco NR-1800 and R-800 spectrometer equipped with a LN-CCD 1152E and a HTV-R649 photomultiplier with Ar^+ or He-Ne laser, or Spectra-Physics R6G dye laser excitation using KBr disk samples sealed in glass tubes under argon atmosphere. IR spectra were recorded on a Jasco FT/IR-3 spectrometer with use of KBr discs. Elemental analyses were performed at Elemental Analysis Center of Osaka University. UV−vis spectra were taken on a Jasco Ubest-30 in a sealed 1 mm cells. All melting points were measured in sealed tubes and were not corrected.

Cyclic Voltammetry and Electrolysis. Cyclic votammetry and electrolyses were carried out with a BAS100B electrochemical workstation referenced to a Ag/AgCl electrode. In the cyclic voltammetry, the working electrode was a glassy-carbon electrode, and the counter electrode was a platinum wire. The measurements were recorded on 1.0 mM dichloromethane solution that contained 0.2 M tetra-*n*-butylammonium perchlorate as supporting electrode at the scan rate of 100 mV/s. Under our experimental conditions the ferrocenium/ferrocene couple was observed at $E_{1/2}$ = 520 mV vs Ag/AgCl.

The electrolysis was performed in stirred dichloromethane solution (1.0 mM) of **7c** containing 0.2 M tetra-*n*-butylammonium perchlorate as supporting electrode. The working electrode and counter electrode were 0.5 × 10 × 20 mm platinum plates. The Ag/AgCl electrode was used as reference electrode.

Crystallographic Data Collections and Structure Determination. Data Collection. Each suitable crystal was mounted in glass capillaries under argon atmosphere. Data for all complexes were collected by a Rigaku AFC-5R diffractometer with a graphite monochromated Mo Kα radiation and a 12 kW rotating anode generator. The incident beam collimator was 1.0 mm, and the crystal to detector distance was 285 mm. Cell constants and an orientation matrix for data collection, obtained from a least-squares refinement using the setting angles of 25 carefully centered reflections, corresponded to the cells with dimensions listed in Tables 9 and 10, where details of the data collection were summarized. The weak reflections ($I < 10\sigma(I)$) were rescanned (maximum of two rescans), and the counts were accumulated to assure good counting statistics. Stationary background counts were recorded on each side of the reflection. The ratio of peak counting time to

(68) (a) Doyle, J. R.; Slade, P. E.; Jonassen, H. B. *Inorg. Synth.* **1960**, *6*, 218. (b) Drew, D.; Doyle, J. R. *Inorg. Synth.* **1972**, *13*, 52. (c) Drew, D.; Doyle, J. R. *Inorg. Synth.* **1972**, *13*, 47.

(69) Newkome, G. R.; Hager, D. C. *J. Org. Chem.* **1978**, *43*, 947.

Table 10. Crystallographic Data of **6** and **7**[a,b]

complex	**6a**	**6b**
formula	$C_{72}H_{60}O_4N_4P_4Mo_2Pd_2Cl_{10}$	$C_{70}H_{56}O_4N_4P_4Mo_2Pd_2Br_2Cl_4$
solvent molecules	dichloromethane (four)	dichloromethane (two)
fw	1928.40	1847.43
cryst system	tetragonal	tetragonal
space group	$I4_1$	$I4_1$
a, Å	17.388(4)	17.455(3)
b, Å		
c, Å	25.748(5)	25.971(6)
β, deg		
V, Å^3	7784(4)	7913(3)
Z	4	4
*D*calc, g cm^{-3}	1.645	1.693
radiation	MoKα	MoKα
temp, K	296	296
linear abs coeff, cm^{-1}	12.32	21.69
cryst. size, mm	0.3 × 0.4 × 0.4	0.6 × 0.6 × 0.6
GOF	1.19	2.09
no. of unique data	5840	3270
no. of data with $I > 3\sigma(I)$	3112	2162
no. of variables	445	445
R	0.032	0.029
R_w	0.035	0.027

complex	**6c**	**7a**
formula	$C_{69}H_{54}O_4N_4P_4Mo_2Pd_2I_2Cl_2$	$C_{72}H_{60}O_4N_4P_4Mo_2Pt_2Cl_{10}$
solvent molecules	dichloromethane (one)	dichloromethane (four)
fw	1856.50	2105.77
cryst system	monoclinic	tetragonal
space group	$P2_1/n$	$I4_1$
a, Å	16.074(7)	17.407(2)
b, Å	16.807(7)	
c, Å	28.194(4)	25.798(3)
β, deg	94.97(2)	
V, Å^3	7587(3)	7817(2)
Z	4	4
*D*calc, g cm^{-3}	1.625	1.789
radiation	MoKα	MoKα
temp, K	296	296
linear abs coeff, cm^{-1}	18.03	43.85
cryst. size, mm	0.4 × 0.4 × 0.5	0.3 × 0.4 × 0.4
GOF	5.28	1.095
no. of unique data	21237	5854
no. of data with $I > 3\sigma(I)$	9689	3319
no. of variables	802	445
R	0.069	0.028
R_w	0.084	0.031

complex	**7b**	**7c**
formula	$C_{69}H_{54}O_4N_4P_4Mo_2Pt_2Br_2Cl_2$	$C_{69}H_{54}O_4N_4P_4Mo_2Pt_2I_2Cl_2$
solvent molecules	dichloromethane (one)	dichloromethane (one)
fw	1939.88	2033.88
cryst system	monoclinic	monoclinic
space group	$P2_1/n$	$P2_1/n$
a, Å	16.077(3)	16.137(3)
b, Å	16.592(3)	16.815(3)
c, Å	27.861(2)	28.274(1)
β, deg	96.10(1)	94.888(8)
V, Å^3	7390(2)	7644(2)
Z	4	4
*D*calc, g cm^{-3}	1.743	1.767
radiation	MoKα	MoKα
temp, K	296	296
linear abs coeff, cm^{-1}	54.13	49.97
cryst. size, mm	0.3 × 0.3 × 0.5	0.4 × 0.5 × 0.5
GOF	1.817	2.22
no. of unique data	22378	23120
no. of data with $I > 3\sigma(I)$	8564	8475
no. of variables	891	920
R	0.053	0.060
R_w	0.069	0.078

[a] $R = \sum||F_o| - |F_c||/|F_o|$. [b] $R_w = [\sum w(|F_o| - |F_c|)^2/\sum wF_o^2]^{1/2}$. $w = 1/\sigma^2(F_o)$; function minimized: $\sum w(|F_o| - |F_c|)^2$.

background counting time was 2:1. Three standard reflections were chosen and monitored every 100 reflections and not shown any significant change in intensity over the data collection period.

Data Reduction. An empirical absorption correction based on azimuthal scans of several reflections was applied. The data were corrected for Lorentz and polarization effects.

Structure Determination and Refinement. The structure of **1**, **6a**, **6b**, **7a**, **7b**, and **7c** were solved by direct methods, MITHRIL, and the structure of **2b** by direct method, SIR88. The structure of **2a**, **4a**, and **6c** was solved by heavy-atom Patterson methods, PATTY. These were expanded using Fourier techniques. Measured nonequivalent reflections with $I > 3.0\,\sigma(I)$ were used for the structure determination. The non-hydrogen atoms were refined anisotropically. The crystal of all compounds contain some solvent molecules, CH_2Cl_2. In the final refinement cycle, hydrogen atom coordinates were included at idealized positions and were given the same temperature factor as that of the carbon atom to which they were bonded. All calculations were performed using a TEXSAN crystallographic software package of the Molecular Structure Corporation.

Preparation of 1. To a mixture of $Mo_2(O_2CCH_3)_4$ (1.31 g, 3.06 mmol), pyphosH (3.42 g, 12.3 mmol), and NaOMe (0.669 g, 12.4 mmol) was added dichloromethane (150 mL). After stirring the mixture for 6 days, the insoluble products were removed by filtration. The solvent was removed *in vacuo*, and the resulting product was recrystallized from dichloromethane−diethyl ether at room temperature to afford **1** as red crystals (2.14 g, 53% yield), mp 140−150 °C (dec). ^{1}H NMR (C_6D_6, 30 °C): δ 6.36 (d, J_{HH} = 6.9 Hz, 4H), 6.58 (d, J_{HH} = 8.7 Hz, 4H), 6.76 (dd, J_{HH} = 6.9 Hz, J_{HH} = 8.7 Hz, 4H), 7.07−7.14 (m, 24H), 7.40−7.46 (m, 16H). ^{31}P{^{1}H} NMR ($CDCl_3$, 30 °C): δ −7.8 (s). FAB-MS for ^{98}Mo *m*/*z* 1309 (MH^+). Anal. Calcd for $C_{68}H_{52}N_4O_4P_4Mo_2$: C, 62.59; H, 4.02; N, 4.29. Found: C, 61.99; H, 4.15; N, 4.28.

Preparation of 2a. A mixture of **1** (0.293 g, 0.225 mmol) and $PdCl_2(PhCN)_2$ (0.174 g, 0.454 mmol) in dichloromethane (60 mL) was stirred for 1 day at room temperature, and then supernatant was removed to give red brown powder (50% yield). ^{1}H NMR ($CDCl_3$, 30 °C): δ 5.95 (d, J_{HH} = 8.1 Hz, 4H), 6.52 (m, 4H), 7.11 (m, 4H), 7.30−7.33 (m, 16H), 7.40−7.50 (m, 24H). ^{31}P{^{1}H} NMR ($CDCl_3$, 30 °C): δ 16.1 (s). Anal. Calcd for $C_{68}H_{52}Cl_4Mo_2N_4O_4P_4Pd_2(CH_2Cl_2)$: C, 47.51; H, 3.12; N, 3.21. Found: C, 47.78; H, 3.11; N, 3.37.

Preparation of 2b. A mixture of $PdBr_2$(cod) (cod = 1,5-cyclooctadiene) (0.050 g, 0.144 mmol) and **1** (0.083 g, 0.064 mmol) in dichloromethane (20 mL) was stirred for a few minutes, and then the solution was left undisturbed at room temperature for 3 days to give brown microcrystals (32% yield). ^{1}H NMR (CD_2Cl_2, 30 °C): δ 6.01 (d, J_{HH} = 8.6 Hz, 4H), 6.18 (m, 4H), 7.17 (m, 4H), 7.22−7.26 (m, 16H), 7.28−7.33 (m, 24H). ^{31}P{^{1}H} NMR ($CDCl_3$, 30 °C): δ 16.5 (s). Anal. Calcd for $C_{68}H_{52}Br_4Mo_2N_4O_4P_4Pd_2(CH_2Cl_2)$: C, 43.11; H, 2.83; N, 2.91. Found: C, 43.16; H, 2.82; N, 3.06.

Preparation of 4a. A mixture of $PtCl_2$(cod) (0.321 g, 0.619 mmol) and **1** (0.404 g, 0.310 mmol) was dissolved in dichloromethane (20 mL). After stirring for 3 days at 40 °C, the supernatant was removed to give quantitatively **4a** as gray powder. ^{1}H NMR ($CDCl_3$, 30 °C): δ 6.49 (t, 4H), 6.73 (d, 4H), 7.20−7.59 (m, 44H). ^{31}P{^{1}H} NMR ($CDCl_3$, 30 °C): δ 12.6 (J_{Pt-P} = 3592 Hz). Anal. Calcd for $C_{68}H_{52}Cl_4Mo_2N_4O_4P_4Pt_2\cdot 6(CH_2Cl_2)$: C, 37.88; H, 2.75; N, 2.39. Found: C, 37.36; H, 3.06; N, 2.87.

A similar procedure was used in the preparation of bromo and iodo complexes.

4b: quantitative yield. ^{1}H NMR ($CDCl_3$, 30 °C): δ 6.52 (t, 4H), 6.72 (d, 4H), 7.20−7.60 (m, 44H). ^{31}P{^{1}H} NMR ($CDCl_3$, 30 °C): δ 12.6 (J_{Pt-P} = 3592 Hz). Anal. Calcd for $C_{68}H_{52}Br_4Mo_2N_4O_4P_4Pt_2$: C, 40.54; H, 2.60; N, 2.78. Found: C, 40.97; H, 3.44; N, 2.43.

4c: quantitative yield. ^{1}H NMR ($CDCl_3$, 30 °C): δ 6.55 (m, 4H), 6.71 (d, 4H), 7.20−7.63 (m, 44H). ^{31}P{^{1}H} NMR ($CDCl_3$, 30 °C): δ 7.9 (J_{Pt-P} = 3383 Hz). The contamination of **7c** prevented elemental analysis.

Preparation of 6a. A mixture of **1** (0.097 g, 0.074 mmol), $PdCl_2(PhCN)_2$ (0.057 g, 0.15 mmol), and Et_4NBH_4 (0.006 g, 0.04 mmol) in dichloromethane (40 mL) was stirred for 2 h at room temperature. All volatiles were removed under reduced pressure to give a deep green solid, and then recrystallization of the resulting solid from dichloromethane−diethyl ether gave **6a** as red crystals in 69% yield, mp 237−243 °C. ^{1}H NMR ($CDCl_3$, 30 °C): δ 6.03 (d, J_{HH} = 8.2 Hz, 4H), 6.25 (d, J_{HH} = 7.0 Hz, 4H), 7.2 (dd, 4H), 7.33−7.46 (m, 24H), 7.50−7.57 (m, 16H). ^{31}P{^{1}H} NMR ($CDCl_3$, 30 °C): δ 15.7 (s). FAB-MS for ^{98}Mo^{106}Pd *m*/*z* 1521 (MH^+-Cl_2). Anal. Calcd for $C_{68}H_{52}Cl_2Mo_2N_4O_4P_4Pd_2(CH_2Cl_2)$: C, 49.52; H, 3.25; N, 3.35. Found: C, 49.97; H, 3.38; N, 3.50.

Preparation of 6b. To a Schlenk tube containing $PdBr_2$(cod) (0.193 g, 0.515 mmol) and **1** (0.265 g, 0.203 mmol) was added dichloromethane (20 mL). After stirring for 14 h at room temperature, all volatiles were removed under reduced pressure to give deep green powder. Recrystallization of the resulting powder from dichloromethane−diethyl ether gave red crystals of **6b** in 63% yield, mp > 300 °C. ^{1}H NMR ($CDCl_3$, 30 °C): δ 6.06 (d, 4H), 6.22 (d, 4H), 7.16 (d, 4H), 7.34−7.47 (m, 24H), 7.50−7.57 (m, 16H). ^{31}P NMR ($CDCl_3$, 30 °C): δ 15.7(s). FAB-MS for ^{98}Mo ^{106}Pd *m*/*z* 1600 ($MH^+ - Br_2$). Anal. Calcd for $C_{68}H_{52}N_4O_4P_4Mo_2Pd_2Br_2$: C, 44.45; H, 2.85; N, 3.05. Found: C, 44.12; H, 3.50; N, 2.76.

By the similar procedure, complexes **6c** and **7a**−**c** were prepared and characterized.

6c: 50% yield, mp > 300 °C. ^{1}H NMR ($CDCl_3$, 30 °C): δ 6.00 (d, 4H), 6.17 (d, 4H), 7.14 (t, 4H), 7.33−7.54 (m, 40H). ^{31}P NMR ($CDCl_3$, 30 °C): δ 15.8 (s). Anal. Calcd for $C_{68}H_{52}N_4O_4P_4I_2Mo_2Pd_2(CH_2Cl_2)$: C, 44.64; H, 2.93; N, 3.02. Found: C, 44.35; H, 3.15; N, 2.91.

7a: 40% yield, mp > 300 °C. ^{1}H NMR ($CDCl_3$, 30 °C): δ 5.77 (d, 4H), 6.21 (m, 4H), 7.15 (m, 4H), 7.34−7.47 (m, 24H), 7.51−7.59 (m, 16H). ^{31}P NMR ($CDCl_3$, 30 °C): δ 27.9 (J_{Pt-P} = 3391 Hz). FAB-MS for ^{98}Mo ^{195}Pt *m*/*z* 1699 ($MH^+ - Cl_2$). Anal. Calcd for $C_{68}H_{52}N_4O_4P_4Mo_2Pt_2Cl_2(CH_2Cl_2)$ C, 44.77; H, 2.94; N, 3.03. Found: C, 45.21; H, 2.95; N, 3.12.

7b: 28% yield, mp > 300 °C. ^{1}H NMR ($CDCl_3$, 30 °C): δ 5.79 (d, 4H), 6.17 (m, 4H), 7.15 (m, 4H), 7.34−7.47 (m, 24H), 7.51−7.60 (m, 16H). ^{31}P NMR ($CDCl_3$, 30 °C): δ 27.3 (J_{Pt-P} = 3363 Hz). FAB-MS for ^{98}Mo ^{195}Pt *m*/*z* 1699 ($MH^+ - Br_2$). Anal. Calcd for $C_{68}H_{52}N_4O_4P_4Mo_2Pt_2Br_2(CH_2Cl_2)$ C, 42.72; H, 2.81; N, 2.89. Found: C, 42.18; H, 2.81; N, 2.89.

7c: 36% yield, mp > 300 °C. ^{1}H NMR ($CDCl_3$, 30 °C): δ 5.77 (d, 4H), 6.13 (m, 4H), 7.15 (m, 4H), 7.34−7.47 (m, 24H), 7.51−7.59 (m, 16H). ^{31}P NMR ($CDCl_3$, 30 °C): δ 26.7 (J_{Pt-P} = 3331 Hz). FAB-MS for ^{98}Mo ^{195}Pt *m*/*z* 1699 ($MH^+ - I_2$). Anal. Calcd for $C_{68}H_{52}N_4O_4P_4Mo_2Pt_2I_2(CH_2Cl_2)_2$ C, 39.68; H, 2.66; N, 2.64. Found: C, 39.49; H, 3.15; N, 2.45.

Complex **7c** was prepared alternatively as follows: To a Schlenk tube containing **1** (215 mg, 0.156 mmol) and PtI_2(cod) (0.186 g, 0.334 mmol) was added dichloromethane (20 mL). After stirring for several days at 30 °C, all volatiles were removed under reduced pressure to give a deep red powder. The resulting powder was placed in an apparatus for sublimation with a cold finger, and then it was heated at 300° C in reduced pressure for 12 h to give a purple solid of **7c** in quantitative yield. In this process, iodine was sublimed on the cold finger.

Acknowledgment. K.M. and A.N. are grateful for financial support from the Ministry of Education, Science and Culture of Japan (Specially Promoted Research No. 06101004).

Supporting Information Available: Final positional parameters, final thermal parameters, bond distances, bond angles, and ORTEP drawings for **1**, **2a**, **2b**, **4a**, **6a**−**c** and **7a**−**c** (75 pages). See any current masthead page for ordering and Internet access instructions.

JA960606G